universität wien

DIPLOMARBEIT / DIPLOMA THESIS

Titel der Diplomarbeit / Title of the Diploma Thesis

„Synthesis of polycationic gene carrier systems and their biophysical evaluation“

verfasst von / submitted by

Jakob Sperhansl

angestrebter akademischer Grad / in partial fulfilment of the requirements for the degree of

Magister der Pharmazie (Mag.pharm.)

Wien, 2016 / Vienna, 2016

Studienkennzahl lt. Studienblatt / degree programme code as it appears on the student record sheet:	A 449
Studienrichtung lt. Studienblatt / degree programme as it appears on the student record sheet:	Diplomstudium Pharmazie UniStG
Betreut von / Supervisor:	Univ.Prof. Dipl. Ing. Dr. Manfred Ogris
Mitbetreut von / Co-Supervisor:	

"We used to think that our fate was in our stars, but now we know that, in large measure, our fate is in our genes. “ (Francis Crick)

Acknowledgements:

Danke an Prof. Manfred Ogris, der mir die Arbeit in seinem Labor ermöglichte. Ihm und allen Mitgliedern des MMCT Lab möchte ich mich für das freundschaftliche, entspannte und dennoch produktive Arbeitsklima bedanken, es war eine richtig schöne Zeit. Besonderer Dank gilt hier vor allem Alexander Taschauer, der mich nicht besser hätte betreuen können. Danke an Karoline Völkers für die Bereitstellung der Plasmide.

Danke an meine Eltern, Johann und Monika, die mir das Studium der Pharmazie ermöglicht haben. Sowohl ihnen als auch meiner Schwester Lisi möchte ich für die Unterstützung danken.

Nicht zuletzt möchte ich mich bei meiner geliebten Laura bedanken, die mich bedingungslos in allen Lebenslagen unterstützt und mir immer mit Rat und Tat zur Seite steht.

Table of Contents

1 Introduction

Since we know that various maladies are attributable to defects in several genes and the whole human genome has been completely sequenced, the focus on gene therapy significantly increased (Lio, 2000).

Already in the early 1960's Szybalska et al. achieved a successful transfer of genetic material into mammalian cells and until now, more than 900 clinical trials related to gene delivery have been conducted (Szybalska, 1962; Cotrim, 2008).

Gene therapy offers new possibilities for the treatment of various diseases such as cystic fibrosis, x-SCID, β–thalassemia and cancer (Matissek, 2011).

8.2 million cases of death in 2012 were caused by cancer and the incidence rate seems to be increasing rapidly. Therefore it is among the most abundant causes of morbidity and mortality (http://www.who.int/mediacentre/factsheets/fs297/en/, 2016). Cancer is considered a genetic disease. Only about 1% of the cases have a hereditary genesis.

Two essential properties determine cancer, namely the ability of proliferation and metastasis (Klug, 2012). These characteristics are mainly based on an accumulation of genetic alterations, in contrast to monogenic diseases where just one mutation in one specific gene leads to pathogenesis. Such mutagenic events mostly occur in tumour-suppressor genes, oncogenes and stability genes leading to increased proliferation and decreased repair of defect genetic material (Vogelstein, 2004).

Tumour suppressors such as p53 control the cell cycle and induce apoptosis. A loss of function in the genes encoding for tumour suppressors results in uncontrolled growth and consequently the emergence of neoplasia (Klug, 2012).

The formation of oncogenes is mainly based on the mutation of protooncogenes whose translational products are responsible for normal growth, cleavage and differentiation of cells. Gain-of-function mutations cause excessive proliferation and in further consequence the development of tumours (Vogelstein, 2004; Klug, 2012).

Considering that cancer is a complex genetic disease makes the thought of an individualized therapy on the genomic level reasonable (Cotrim, 2008).

Currently standard therapy of solid carcinoma is surgery followed by radiotherapy and chemotherapy. But high toxicity of radio- and chemotherapeutics as well as resistance mechanisms of cancer cells often limit the successful treatment of the disease (Rödl, 2013).

In respect of nucleic acid based therapy of cancer two major strategies can be performed: On the one hand, RNA interference (RNAi) can be used to inhibit the translation from specific messenger RNA (mRNA) into corresponding proteins. On the other hand it is possible to use plasmid DNA (pDNA) which is translated into cytotoxic proteins such as TNFα or prodrug converting enzymes. However, both approaches offer high selectivity (Collet, 2013; Schaffert, 2013; Su, 2013).

Another strategy is the expression of the sodium/iodide symporter (NIS) in tumour cells allowing influx and accumulation of radioiodine and thus the imaging of the tumour using radio-medicinal methods (Klutz, 2009).

1.1 Delivery of nucleic acids

Due to general properties of nucleic acids generation of delivery systems is necessary. The anionic characteristic of the biopolymers' backbones hampers the uptake through the cellular membrane and results in interactions with blood components. This together with their high molecular weight and their sensibility towards decomposition through nucleases are the principal barriers (Gehrig, 2014).

So there are several delivery strategies that can be followed to overcome those obstacles. One possibility is the use of viral nucleic acid carrier systems. Viruses are highly evolved protein machineries with the ability to efficiently transfect cells with either RNA or DNA (Gehrig, 2014). In addition reoviruses show oncolytic activity. Reoviruses interfere with highly active pathways of tumour cells (Collet, 2013).

A big downside of viral vectors are the immunological responses such as the neutralisation via antibodies often occurring after repeated administration.

Non-viral gene delivery vehicles show advantages like a well-defined and modifiable structure. However, compared to viral vectors non-viral gene delivery agents are also characterized by relatively low transfection efficiency (Gehrig, 2014).

Figure 1 *Scheme of complex formation between a positively charged polymer and negatively charged DNA (figure from Akhtar et al., 2006)*

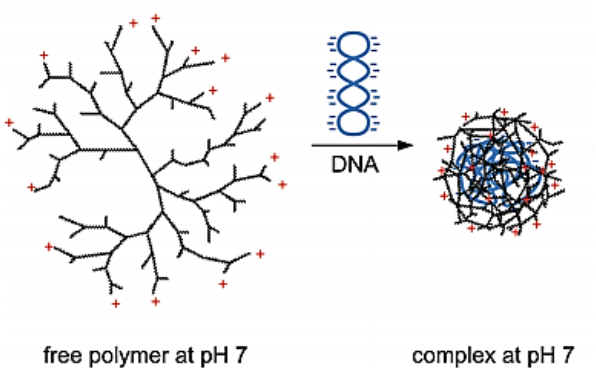

For non-viral gene delivery a broad variety of approaches is available. Besides the integration of nucleic acids into liposomes or exosomes using cationic lipids peptidic coumpounds like poly-L-lysine and positively charged polymers like polyethylenimine can be used to deliver nucleic acids to their site of action. Those positively charged polymers complex nucleic acids into compact nanoparticles due to electrostatic interactions and therefore protect them from enzymatic degradation (Figure 1) (Collet, 2013). These polymeric derived particles are also called as polyplexes.

Due to a surplus of positive charge these polyplexes are internalized into cells by absorptive endocytosis after electrostatic interaction with negatively charged molecules on the cellular membrane (Nguyen, 2012; Schaffert, 2013).

The endosomal release of polyplexes is described in the hypothesis of a proton sponge effect. ATP driven proton pumps are carrying protons into the endosome, leading to acidification. Normally this would result in the fusion of the endosomes with lysosomes when an approximate pH of 5 is reached which would finally end in the enzymatic degradation of the content. But due to the considerable buffer capacity of these polyamines the endosomal acidification is prevented. This results in an intra-endosomal accumulation of protons, triggering an increased influx of chloride ions and water leading to vesicular rupture and the release of the vector into the cytosol (Figure 2) (Nguyen, 2012; Schaffert, 2013).

Figure 2 *Schematic representation of the proton sponge effect (figure from Akhtar et al., 2006)*

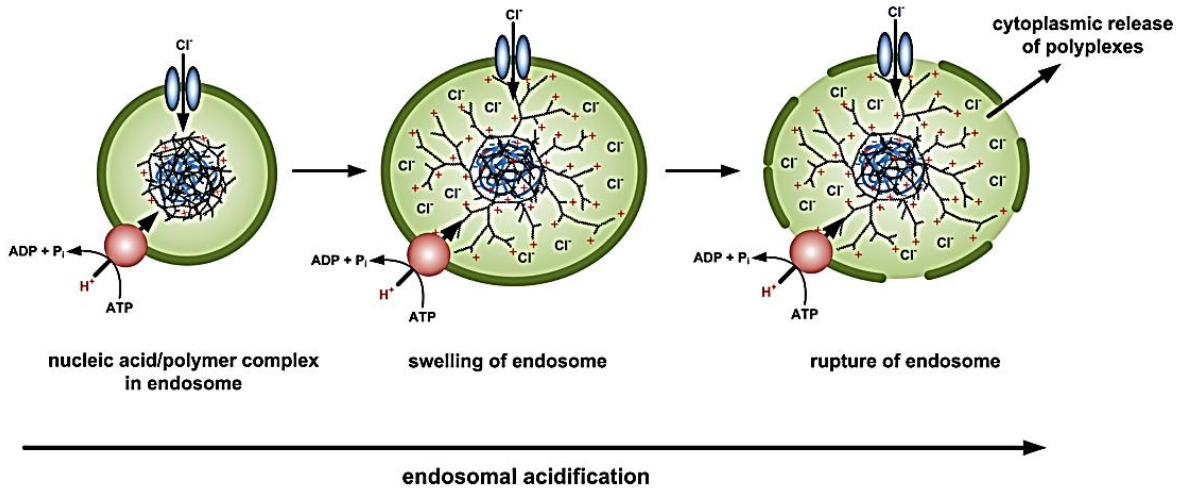

1.2 Polyethylenimine based nucleic acid carriers

Polyethylenimine (PEI) is a gold standard for non-viral gene delivery. There are two different forms of PEI available, namely branched (BPEI) and linear polyethylenimine (LPEI). Their protonable amine groups cause a high density of positive charges enabling electrostatic interaction with the negatively charged backbone of nucleic acids followed by a hydrophobic collapse (Rödl, 2013). Properties like size, ζ-potential and transfection efficiency of the resulting polyplexes are dependent on the ratio between amino groups of the polymer and phosphate groups of the nucleic acid, also termed as N/P-ratio. The higher this ratio is the more positive is the surface charge of the complexes (Kichler, 2004).

Although the synthesis of polyethylenimine is known since the 1950's, its ability to work as nucleic acid delivery system was discovered approximately 20 years ago (Jones, 1944; Boussif, 1995).

BPEI contains primary as well as secondary and tertiary amines. It is synthesized by an acid catalysed cationic ring opening polymerization (CROP) of ethylenimine (aziridine) initiated by an electrophilic attack on the ethylenimine monomer (Figure 3).

Figure 3 *Mechanism of BPEI synthesis (Schaffert, 2013)*

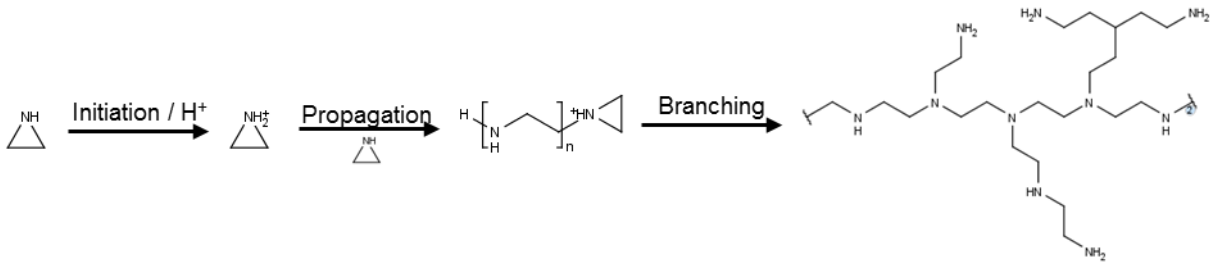

The generated aziridinium ion is highly reactive and can both be attacked by aziridine monomers or PEI chains leading to a branched polymeric structure. The consequence resulting from this reaction mechanism is a loss of control regarding the structure leading to batch to batch variability (Schaffert, 2013).

In contrast to that linear polyethylenimine (LPEI) only consists of secondary amino groups. Its synthesis is based on using poly-2-acyl-2-oxazoline as initial compound which is formed by cationic ring-opening polymerization of 2-acyl-2-oxazoline, initiated by electrophilic attack. Deacylation by acidic hydrolysis of poly-2-acyl-2-oxazoline results in obtaining LPEI (Figure 4).

Figure 4 *Mechanism of LPEI synthesis (Schaffert, 2013)*

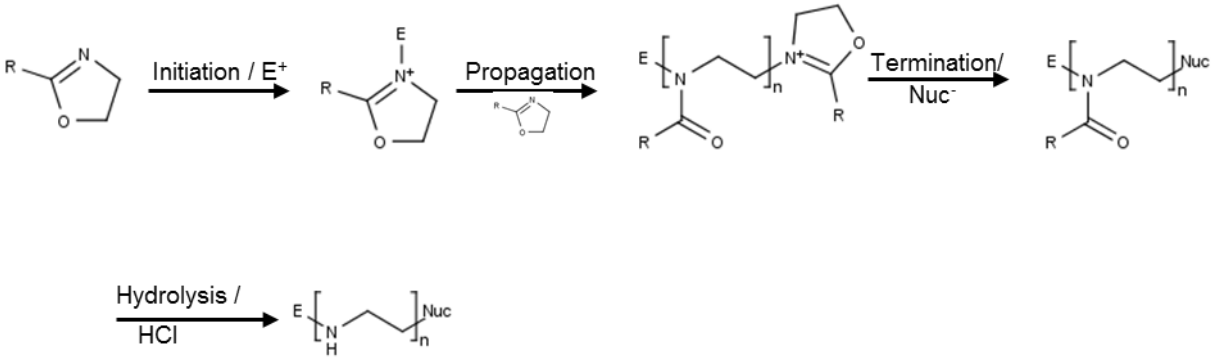

Also regarding transfection *in vitro* and *in vivo* linear polyethylenimine is more efficient compared to BPEI. It is the lower complexation strength of LPEI based polyplexes in comparison to their BPEI based polyplexes which leads to a more efficient release of the nucleic acid thus to a greater transfection efficiency (Rödl, 2013).

Intravenous administration of LPEI based polyplexes into the tail vein of mice leads to gene expression mainly in lung tissue. The nanoparticular vectors are able to transfect pneumocytes and alveolar cells (Wightman, 2001). For efficient transfection of pulmonary tissue two major requirements are necessary - the aggregation of polyplexes with blood platelets and the occurrence of free, unbound LPEI (Boeckle, 2004; Chollet, 2002; Rödl, 2013). Additionally, a significant amount of the LPEI derived nanoparticles reallocate to the liver, in contrast to BPEI polyplexes (Schaffert, 2013).

1.3 Modification of LPEI

1.3.1 Reduction of cytotoxicity

One major disadvantage of LPEI is its high cytotoxicity (Schaffert, 2013). This characteristic is mainly ascribable to non-specific ionic interaction of LPEI with the cellular membrane which leads to breakdown of membrane potential, reduction of cytoplasmic proteins and consequently to cell death (Fischer, 2003). Additionally interference with intracellular pathways leads to oxidative stress, inflammation and cytotoxicity (Regnstrom, 2006; Breunig, 2007).

It is also shown that cytotoxicity of LPEI based polyplexes correlates with the N/P-ratio and the molecular weight of the polymer. While polyplexes based on LPEI with low molecular weight (<2 kDa) exhibit low cytotoxicity its ability to transfect cells is relatively low compared to LPEI with higher molecular weight (Breunig, 2007). The reason lies in a lower buffering capacity as well as in the decreased colloidal stability and strength of electrostatic interactions (Boeckle, 2004; Breunig, 2007; Schaffert, 2013).

Crosslinking of low molecular weight LPEI with disulfide bonds using biodegradable linkers such as Lomant's reagent (3,3'-Dithiodipropionicaciddi(N-succinimidylester)) and boc protected cystine results in products characterized by high transfection efficiency combined with lower cytotoxicity. The main problem which occurs by using such crosslinkers is the uncontrollable introduction of inter- and intramolecular connections (Breunig, 2007).

1.3.2 Improving biocompatibility

Polyethylenimine based polyplexes have the tendency to interact with plasmatic components and erythrocytes leading to aggregation and accumulation in the lung. By conjugation of PEI with the hydrophilic polymer polyethylene glycol (PEG) the circulation time can be increased due to "stealth" characteristics of PEG. It was also shown that cytotoxicity of PEG bound polyethylenimines is reduced (Schafer, 2011). However, the reduced surface charge results in lower transfection efficiency due to

decreased cellular uptake. This effect is generally known as the “PEG-dilemma” (Kichler, 2004; Rinkenauer, 2015).

1.3.3 Targeting to specific tissue/tumours

As stated previously, polyplexes are interacting unspecifically with cell membranes due to a surplus of positive charge on their surface. To achieve more specificity towards other tissues the nanocarriers can be modified with targeting ligands triggering receptor mediated endocytosis. There is a broad range of ligands available such as sugar moieties, antibodies or peptidic ligands (Kichler, 2004).

PEI/DNA complexes conjugated with Galactose-residues, for example, are able to specifically bind asialoglycoprotein receptor on hepatocytes. Kircheis et al. have shown, that polyplexes coupled with transferrin showed high reporter gene expression in tumour tissue, since its receptor is upregulated in various tumours. Another advantage of transferrin coupled to polyplexes is the shielding of positive charges due to its relatively big size analogous to the “stealth” strategy with polyethylene glycol (Kircheis, 2001; Kichler, 2004; Schaffert, 2013).

A reasonable approach is the combination of specific targeting with the already described “stealth” strategy based on PEGylation (Kichler, 2004).

A very promising target is the epidermal growth factor receptor (EGFR, ERBB1 or HER1) which is overexpressed in a broad range of solid tumours such as breast, lung, liver and bladder cancer and glioblastoma. Binding of epidermal growth factor (EGF) to EGFR promotes cell proliferation and cell migration. Therefore using EGF as a targeting molecule for anti-tumour therapy is not recommendable (Schafer, 2011).

The synthetic peptide YHWYGYTPQNVI also termed as GE11 is able to bind EGFR without activating the receptor (Li, 2005). It is shown that LPEI based conjugates containing GE11 as targeting residue exhibit high transfection efficiency in EGFR upregulated tumour types both *in vitro* and *in vivo (Schafer, 2011)*. Synthesis of LPEI based conjugates with a targeting residue can be accomplished by using polyethylene glycol as heterobifunctional linker. For this purpose PEG functionalized with N-hydroxysuccinimide (NHS) on one terminus and an ortho-pyridyldithio moiety (OPSS) on the other terminus is used for connecting an amino group in LPEI with a mercapto

group in the targeting peptide. The NHS group forms stable amid bonds with the nitrogen atoms of LPEI. Then, via formation of reducible disulphide bonds between the N-terminal cysteine in the peptide and the OPSS group the conjugation of GE11 is obtained (Schafer, 2011; Schaffert, 2013).

1.4 Nanoparticle tracking analysis

The size of LPEI/pDNA complexes correlates with transfection efficiency (Behr, 1989; Wightman, 2001). However, polyplexes formed with LPEI (22 kDa) in salt free media remain rather small and exhibit good transfection efficiency *in vivo*, while increasing the salt concentration of the buffer leads to aggregation of the particles (Wightman, 2001). Also the surface charge is an important characteristic of nanoparticles because of its influence on the transfection abilities of polyplexes and on the interaction between nanoparticles and blood components (Kichler, 2004).

Thus, investigation of both size and ζ-potential is necessary for quality control of nanoparticles. Diffuse light scattering (DLS) systems are routinely used to measure size and ζ-potential of nanoparticles. Size is calculated based on Brownian motion of particles in the media determined by fluctuations of the scattered light (Filipe, 2010). ζ-potential is determined by using laser Doppler microelectrophoresis (http://www.malvern.com/de/products/product-range/zetasizer-range/zetasizer-nano-range/zetasizer-nano-zsp/default.aspx, 2015). However, DLS suffers from major drawbacks mainly attributable to the principle of taking measurements. Because the intensity of the scattered light is proportional to the sixth potency of the hydrodynamic diameter larger particles like dust or aggregates can hamper the determination of the size (Filipe, 2010). Furthermore the resolution of measurements is relatively low compared to techniques like nanoparticle tracking analysis (NTA). Only 3 fold differences in size or higher are displayed as different peaks in DLS measurements (Filipe, 2010).

Nanoparticle tracking analysis which was first commercialized in 2006 can be an improvement. The main difference to DLS is the optical system and the visualisation of particles. A laser beam is led through a measuring chamber where it gets refracted by glass and liquid. Particles passing the chamber are scattering this beam. The scattered light is then gathered by a scientific complementary metal-oxide semiconductor (sCMOS) camera aligned in a 90 degree angle to the chamber capturing individual particles by their refractive index (Figure 5). Videos are captured and then analysed (http://www.malvern.com/de/products/product-range/nanosight-range/nanosight-ns500/default.aspx, 2015; Carr, 2008; Filipe, 2010).

The measuring principle of NTA lies in the detection of the Brownian motion of every single particle. Size is calculated employing the Stokes-Einstein equation using the Boltzmann constant k_B, mean speed ($\overline{(x, y^2)}$) and the hydrodynamic radius (r_h) of each particle at a certain temperature (T) as well as the viscosity (η) of the medium (Filipe, 2010):

$$\overline{(x, y^2)} = \frac{2k_B T}{3r_h \pi \eta}$$

ζ-potential is determined by measuring the electrophoretic mobility after voltage is applied (http://www.malvern.com/de/products/product-range/nanosight-range/nanosight-ns500/default.aspx, 2015; Carr, 2008). NTA shows several advantages compared to DLS such as high resolution measurements which makes it useful for analysing samples characterized by high polydispersity. Only a 0.5 fold difference in the hydrodynamic diameter is needed for NTA measurement for differentiating between two different particle populations (Filipe, 2010).

Figure 5 *Scheme of the optical system used for nanoparticle tracking analysis (figure from http://www.malvern.com/de/products/product-range/nanosight-range/nanosight-ns500/default.aspx, 2015).*

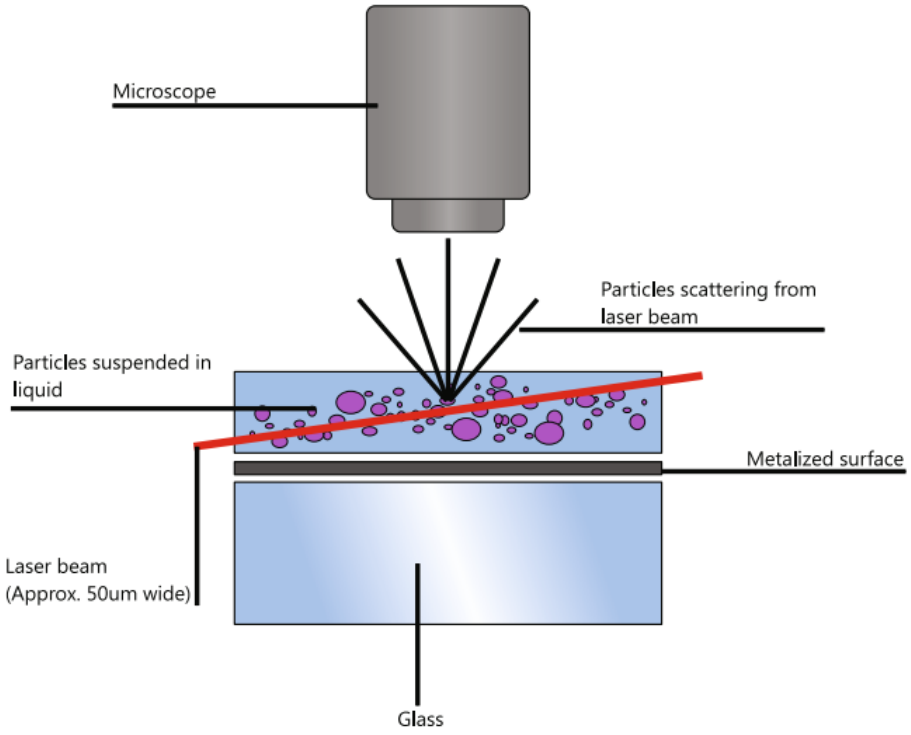

2 Aim of the Thesis

1. In this diploma thesis one of our aims was the synthesis of poly(2-ethyl-2-oxazoline) with different polymerization degrees as initial substance for linear polyethylenimine.

2. Linear polyethylenimine was synthesized via acid hydrolysis of poly(2-ethyl-2-oxazoline).

3. A heterobifunctional linker (NHS-PEG-OPSS) was used to couple LPEI to L-Cysteine. L-Cysteine was chosen instead of a targeting peptide for optimizing the method since the reaction mechanism is the same.

4. Additionally to flash pipetting we wanted to optimize an up-scaled strategy for polyplex synthesis. We used a strategy based on literature of Kasper et al and used a KD scientific LEGATO 210 syringe pump (Kasper, 2011). The LPEI and plasmid DNA (pDNA) containing solutions were mixed in a tubing system (Kasper, 2011).

5. One of our main goals was to investigate size and ζ-potential of polyplexes generated at different N/P ratios, pDNA concentrations, and incubation time points by NTA. The influence of the buffer system on polyplex properties was also investigated.

6. We attempted to make polyplexes visible in particle containing media via NTA by staining LPEI with fluorescein 5(6)-isothiocyanate and use the fluorescence filter of the NanoSight NS500.

3 Materials and Methods

3.1 Chemicals

Table 1 *List of chemicals*

Chemicals	***Supplier***	***Cat.No.***	***Abbreviation***
(2-Hydroxypropyl)-β-cyclodextrin	Sigma Aldrich	H107-5G	
(ortho-pyridyl)disulfide-polyethylene glycol-succinimidyl ester	Rapp Polymere		NHS-PEG-OPSS
2-Ethyl-2-oxazoline	Sigma Aldrich	137456-100ML	
3-(Trimethylsilyl)propionic-2,2,3,3-d4 acid sodium salt	Sigma Aldrich	269913-1G	TMS
4′,6-Diamidino-2-phenylindole dihydrochloride	Sigma Aldrich	D9542-5MG	DAPI
Acetic acid	Sigma Aldrich	320099-500ML-D	
Acetonitrile	Sigma Aldrich	34967-1L	CH_3CN
Calcium hydride	Sigma Aldrich	208027-100G	CaH_2
Chloroform-d	Sigma Aldrich	151823-100G	$CDCl_3$
Copper sulfate pentahydrate	Sigma Aldrich	12849-1KG	
D(+)-Glucose	Merck	108.371.000	
Deuterium oxide	Sigma Aldrich	151882-100G	D_2O

Dichloromethane	Sigma Aldrich	34856-2.5L	CH_2Cl_2
Diethyl ether	Roth	AE04.1	
Dimethyl sulfoxide	VWR	83.673.230	DMSO
Ethanol absolute	Merck	1.117.272.500	EtOH (abs.)
Fluorescein 5(6)-isothiocyanate	Sigma Aldrich	46950-50MG-F	FITC
Hydrochloric acid, fuming	Sigma Aldrich	30721-2.5L-GL-D	HCl (conc.)
L-Cysteine	Sigma Aldrich	168149-100G	
Linear polyethylenimine, Mw= 3/8/10 kDa	Kindly provided by Alexander Taschauer		LPEI 3/8/10 kDa
Methyl p-toluenesulfonate	Sigma Aldrich	158992-100G	MeTOS
N-(2-Hydroxyethyl)-piperazinyl-N'-2-ethanesulfonic Acid	Applichem	A3724,0500	HEPES
pCMV-Gluc	New England Biolabs		
pCpG-hCMV-EF1α-LucSH	first described by Magnusson et al. (Magnusson, 2011)		
RPMI-1640 Medium	Sigma Aldrich	R8758-500ML	
Sodium acetate	Applichem	A4555,0250	
Sodium carbonate	Applichem	A3900,0500	Na_2CO_3

Sodium chloride	Applichem	A2942,5000	NaCl
Sodium hydrogencarbonate	Applichem	A0384,0500	$NaHCO_3$
Sodium hydroxide	Applichem	A6829,1000	NaOH

3.2 Supplies

Table 2 *List of supplies*

Supply	Supplier	Cat.No.
MacroPrep® HighS resin	Bio-Rad	1560030
Molecular sieve (3Å)	Sigma Aldrich	02573-1KG
Ultrapure water (dd H_2O)	obtained using Arium Pro VF ® (Sartorius)	
Spectra/Por® Dialysis Membrane Standard RC (regenerated cellulose) Tubing	Spectrum Labs	132660
Cellulose acetate filter 0.2 µm pore size	VWR	28145-477

3.3 Equipment

Following equipment was used in this thesis:

- NanoVue® UV/Visible spectrophotometer
- GeneQuant® 1300 UV/Visible cuvette spectrophotometer
- PL-GPC 50 Plus system equipped with PL aquagel-OH 30 (8 µm)
- Bruker NMR spectrophotometer Avance 200 MHz
- Christ Alpha 2-4 freeze drying system
- Äkta pure® system (GE Healthcare)
- KD scientific, LEGATO 210 syringe pump
- NanoVue plus (GE Healthcare)
- NanoSight NS500 (Malvern)
- Olympus® IX 7 inverted system microscope

3.4 Reagents

20mM HEPES buffer, pH 7.4:

2,3831 g HEPES (20 mM) were dissolved in 400 ml dd H_2O. pH was then adjusted to 7.4 with hydrochloric acid and sodium hydroxide. The solution was filled up to 500 ml with ddH_2O. The solution was passed through a 0.22 µm filter and stored at room temperature.

HEPES 20mM + 3M NaCl buffer, pH 7.4:

2,3831 g HEPES (20 mM) and 87.66 g sodium chloride (3 M) were dissolved in 400 ml dd H_2O. pH was then adjusted to 7.4 with hydrochloric acid and sodium hydroxide. The solution was filled up to 500 ml with ddH_2O. The solution was passed through a 0.22 µm filter and stored at room temperature.

20mM HEPES + acetonitrile (10% v/v) buffer, pH 7.4:

2,3831 g HEPES (20 mM) and 50 ml acetonitrile (10% (V/V)) were dissolved in 400 ml dd H_2O. pH was then adjusted to 7.4 with hydrochloric acid and sodium hydroxide. The solution was filled up to 500 ml with ddH_2O. The solution was passed through a 0.22 µm filter and stored at room temperature.

20mM HEPES + 3M NaCl + acetonitrile (10% v/v) buffer, pH 7,4:

2,3831 g HEPES (20 mM), 87.66 g sodium chloride (3 M) and 50 ml acetonitrile (10% (V/V)) were dissolved in 400 ml dd H_2O. pH was then adjusted to 7.4 with hydrochloric acid and sodium hydroxide. The solution was filled up to 500 ml with ddH_2O. The solution was passed through a 0.22 µm filter and stored at room temperature.

HEPES buffered glucose (HBG) pH 7.4:

2,3831g HEPES (20 mM) and 25 g glucose (5% (w/V)) were dissolved in 400 ml dd H_2O. pH was then adjusted to 7.4 with hydrochloric acid and sodium hydroxide. The solution was filled up to 500 ml with ddH_2O. The solution was passed through a 0.22 µm filter and stored at room temperature.

HEPES buffered saline (HBS) pH 7.4:

2,3831g HEPES (20 mM) and 4,383 g sodium chloride (150 mM) were dissolved in 400 ml dd H_2O. pH was then adjusted to 7.4 with hydrochloric acid and sodium hydroxide. The solution was filled up to 500 ml with ddH_2O. The solution was passed through a 0.22 µm filter and stored at room temperature.

Copper assay reagent:

0.8203 g sodium acetate were dissolved in 80 ml ddH_2O and the pH was adjusted to 5.5 with acetic acid. The solution was filled up to 100 ml with ddH_2O. Afterwards 23 mg copper sulfate pentahydrate was added.

0.1 M sodium carbonate/bicarbonate buffer:

5.2994 g (0.1 M) sodium carbonate and 4.2004 g (0.1 M) sodium bicarbonate were dissolved in 500 ml dd H_2O, respectively.

0.1 M sodium carbonate/bicarbonate buffer (pH 9) was prepared by adjusting pH of 0.1 M sodium bicarbonate with 0.1 M sodium carbonate.

3.5 Quantification of LPEI stock solutions:

Chemicals needed for protocol:

- **Linear polyethylenimine (LPEI)**
- **Copper assay reagent**

This protocol was used for LPEI containing solutions with a concentration between 0 and 100 µg/ml.

250 µl of copper assay reagent was mixed with 250 µl of LPEI containing solution. 250 µl of the $CuSO_4$ solution mixed with 250 µl solvent used for dissolving LPEI was taken as blank. After incubation for 5 minutes at room temperature absorption was measured at 285 nm. Samples were always prepared in duplicates. The concentration was calculated using a standard curve.

3.6 Synthesis of Poly (2-ethyl-2-oxazoline) (PEtOx)

Chemicals needed for synthesis:

- **2-Ethyl-2-oxazoline**
- **Calcium hydride (CaH_2)**
- **Methyl p-toluenesulfonate**
- **Acetonitrile stored over molecular sieve (3 Å)**
- **Dichloromethane (CH_2Cl_2)**
- **Diethyl ether**

Poly(2-ethyl-2-oxazoline) with different molecular weights enlisted in Table 3 was synthesized as per the protocol of Lungwitz et al. (Lungwitz, 2006) The precursor of linear polyethylenimine namely poly(2-ethyl-2-oxazoline) (pEtOx) was synthesized by cationic ring opening polymerization of the initial substance 2-ethyl-2-oxazoline (2-Et-2-Ox). The reaction was carried out under water-free conditions. Therefore the glassware used during the synthesis was dried in a compartment drier at 150 °C for 3 h prior to use.

2-Ethyl-2-oxazoline was dried over calcium hydride under reflux overnight in argon atmosphere and distilled under vacuum. A stock solution of 2.100g methyl tosylate in 75ml acetonitrile (MeCN) was prepared and stored over a molecular sieve with a pore diameter of 3 Å.

MeTOS stock solution was added to a solution of dry 2-ethyl-2-oxazoline in acetonitrile in a round bottom flask under argon atmosphere (specific amounts see Table 3). The mixture was stirred under reflux (95 °C). The end point of the polymerization was determined by ^{1}H-NMR.

Reaction kinetics were analysed during the synthesis of poly(2-ethyl-2-oxazoline) with a molecular weight of 11.985 kDa. Therefore ^{1}H-NMR samples were taken after 30, 90, 150, 210, 270 and 330 minutes and after 21.75 hours.

After reaching complete conversion of 2-ethyl-2-oxazoline the mixture was cooled down to room temperature and the solvent was evaporated under reduced pressure using a rotavapor system. The residue was redissolved in dichloromethane. The polymer was precipitated with ice cold diethyl ether. After filtration the product was washed 3 times with approximately 5 ml ice cold diethyl ether and dried overnight in a

desiccator. The white to slightly yellow polymer was then analysed by ^{1}H-NMR and gel permeation chromatography (GPC).

^{1}H-NMR samples were prepared using approximately 25 mg of the polymer dissolved in 1 ml deuterated chloroform ($CDCl_3$).

GPC analysis was carried out using a PL aquagel-OH 30 (8 µm) column. 0.1M $NaNO_3$ / 0.07% (w/V) NaN_3 was used as mobile phase. Samples were prepared at a concentration of 1 mg/ml. The flowrate was set to 0.7 ml/min. The standard curve was created using polyethylene glycol standards.

Table 3 *Specific amounts of substances used for poly (2-ethyl-2-oxazoline) synthesis*

M_n of PEtOx [kDa]	**2-Et-2-Ox [ml]**	**2-Et-2-Ox [mmol]**	**MeTOS-MeCN stock [ml]**	**MeTOS [mg]**	**MeTOS [mmol]**	**MeCN [ml]**
15.706	3.1	30.71	9.0	248	1.335	0
13.995			2.6	71	0.385	7
11.985			1.8	49.5	0.265	7.5
5.937			0.9	25	0.135	8.5

3.7 Synthesis of LPEI

Chemicals needed for synthesis:

- **Poly(2-ethyl-2-oxazoline) 15.706 kDa (PetOx)**
- **Hydrochloric acid (HCl conc.)**
- **Sodium hydroxide (NaOH)**
- **ddH_2O**

Synthesis of LPEI was conducted as per instructions of Rödl et al. (Rodl, 2013).

0.601 g (40.067 µmol) PEtOx were dissolved in 38 ml 7 M HCl (22 ml HCl conc. + 16 ml dd H_2O). The mixture was stirred overnight under reflux at 130 °C. LPEI started to precipitate as hydrochloride salt after 3 h.

The product was filtrated and washed four times with 30 ml 7 M HCl. After redissolving in 30 ml of H_2O the product was lyophilized. (yield [LPEI 6.8 kDa-HCl]: 230 mg)

230 mg LPEI 6.8 kDa-HCl was dissolved in 55 ml 1 M NaOH at 100°C. The solution was cooled down to room temperature. LPEI precipitated as free base. The precipitate was filtered and washed three times with 30 ml 1 M NaOH and three times with 30 ml with dd H_2O. The precipitate was resuspended in 30 ml ddH_2O and lyophilized. The product was stored protected from light at room temperature in a desiccator (yield [LPEI 6.8 kDa]: 192 mg).

The product was analysed by ^1H NMR.

3.8 Synthesis and purification of $LPEI_{10kDa}$-PEG-OPSS

Chemicals needed for synthesis:

- **Linear polyethylenimine 10 kDa (LPEI 10 kDa)**
- **Ethanol absolute (EtOH)**
- **NHS-PEG(2 kDa)-OPSS**
- **Dimethyl sulfoxide (DMSO)**
- **N-(2-Hydroxyethyl)-piperazinyl-N'-2-ethanesulfonic Acid (HEPES)**
- **Sodium chloride (NaCl)**
- **Hydrochloric acid (HCl)**
- **ddH_2O**
- **Deuterium Oxide (D_2O)**

The synthesis of LPEI-PEG-OPSS conjugate was carried out as described in the protocol of Rödl et al. (Rodl, 2013).

45.40 mg (4.54 µmol) of LPEI (10 kDa) with a molecular weight of 10 kDa were dissolved in 1.5 ml absolute ethanol. The solution was incubated on a lab mixer at 35 °C for 15 minutes at 800 rpm.

18.60 mg (9.3 µmol; 2 eq.) NHS-PEG-OPSS were dissolved in 100 µl DMSO. The solution was added to the ethanolic solution of LPEI. The mixture was then incubated on a lab mixer at 35°C for 3 hours at 800 rpm.

The reaction mixture was transferred into a 15 ml tube.1 ml 20 mM HEPES buffer (pH 7.4) and 0.84 ml of 20mM HEPES/3M NaCl buffer (pH 7.4) were added. pH was adjusted to 7 using 1 M HCl. Adding 1 M HCl was conducted under constant vortexing to avoid local acidification which would result in precipitation of LPEI. The reaction mixture was then filled up with 20 mM HEPES buffer (pH 7.4) to a total volume of 5 ml to reach a final sodium chloride concentration of 0.5 M.

For purification an Äkta pure® system (GE Healthcare) equipped with a column (10/10) filled with cation exchange resin (MacroPrep® High S) was used. The UV absorption was measured at 240 nm, 280 nm and 343 nm. The system was equilibrated with 83.3% of a 20 mM HEPES solution (pH of 7.4) (solution A) and 16.7% of a solution of and 20 mM HEPES/3 M sodium chloride (pH 7.4) (solution B). The flowrate was set to 0.5 ml/minute. A gradient was programmed as follows:

- 83.3 % of solution A and 16.7 % of solution B from 0 to 25 minutes,
- linear change to 100 % solution B over 40 minutes and
- 100 % solution B for 20 minutes

Fractions eluting within the first 25 minutes contained unreacted NHS-PEG-OPSS linker and by-products from the reaction. Fractions eluting between 2.0 M and 2.8 M sodium chloride contained the conjugate. These fractions were pooled, dialyzed overnight against 5 l ddH_2O at 4°C under constant stirring using a Spectra/Por® dialysis membrane standard RC (regenerated cellulose) tubing with a molecular weight cut off of 6-8 kDa. The solution was snap frozen at -80°C and lyophilized. The product was stored at -80 °C. (yield [LPEI-PEG-OPSS]: 49 mg)

To evaluate the ratio between LPEI and PEG in the conjugate approximately 0.25 g LPEI-PEG-OPSS was dissolved in 2 ml D_2O and analysed by ^{1}H-NMR (200 MHz).

Via ^{1}H-NMR, a ratio of 1.07 PEG molecules per LPEI was calculated.

3.9 Synthesis of $LPEI_{10kDa}$-PEG-Cysteine

Chemicals needed for synthesis:

- **$LPEI_{10kDa}$-PEG-OPSS**
- **N-(2-Hydroxyethyl)-piperazinyl-N'-2-ethanesulfonic acid (HEPES)**
- **Acetonitrile**
- **L-Cysteine**
- **Sodium chloride**
- **ddH_2O**

Coupling of L-cysteine to $LPEI_{10kDa}$-PEG-OPSS was carried out as described by Rödl et al. (Rodl, 2013).

For the reaction an optimal concentration of 4 to 5 mg LPEI-PEG-OPSS per ml is needed. 22.65 mg of LPEI-PEG-OPSS (correlates to 2.4235 µmol PEG-OPSS) were dissolved in 4 ml 20 mM HEPES/10% acetonitrile (pH 7.4). The solution was purged with argon.

0.59 mg (4.85 µmol) L-cysteine dissolved in ddH_2O was added.

The reaction mixture was stirred at room temperature. The absorption of released thiopyridone was measured every 30 minutes at 343 nm. The reaction was left until no change in absorption was observed.

After reaching the endpoint of the reaction 830 µl of 20 mM HEPES/3 M NaCl/10% acetonitrile was added. pH was adjusted to 7. The mixture was then filled up with 20 mM HEPES/10% acetonitrile to a total volume of 5ml, resulting in a final concentration of 0.5 M sodium chloride

For purification an Äkta pure® system (GE Healthcare) equipped with a column (10/10) filled with cation exchange resin (MacroPrep High S®) was equilibrated with 83.3 % 20 mM HEPES/10% acetonitrile (elution buffer A) and 16.7 % 20 mM HEPES/10% acetonitrile/3 M NaCl (elution buffer B). A flowrate of 0.5 ml/minute was set. A gradient was programmed as follows:

- elution with elution 16.7% buffer B for 60 minutes,
- linear increase of elution buffer B up to 100% within the next 30 minutes
- elution with 100% elution buffer B for 30 minutes.

The conjugate was eluted between a NaCl concentration of 2.0 M and 2.8 M. The product containing fractions were pooled and dialyzed against 5 l dd H_2O overnight under constant stirring at 4°C. For Dialysis a Spectra/Por Dialysis Membrane Standard RC Tubing with a molecular weight cut off of 6-8 kDa was used. The product was snap frozen at -80°C, lyophilized and stored at -80 °C. (yield [LPEI-PEG-Cys]: 18 mg)

3.10 Coupling of LPEI with fluorescein isothiocyanate

Chemicals needed for synthesis:

- **Linear polyethylenimine (LPEI) 10 kDa**
- **Linear polyethylenimine (LPEI) 8 kDa**
- **Linear polyethylenimine (LPEI) 3 kDa**
- **Carbonate/bicarbonate buffer, pH 9**
- **Hydrochloric acid (HCl)**
- **Sodium hydroxide (NaOH)**
- **Fluorescein isothiocyanate (FITC)**
- **Dimethyl sulfoxide (DMSO)**
- **dd H_2O**

LPEI with a molecular weight of 3 kDa, 8 kDa and 10 kDa were all labelled using the following protocol:

LPEI was dissolved in 100 ml 0.1 M carbonate/bicarbonate buffer (pH 9) at a concentration of 2 mg/ml.

FITC (25 eq.; 8 mg; 20.55 mmol) dissolved in 100 µl DMSO was added. The mixture was stirred overnight at room temperature protected from light for 48 h. The mixture was then dialyzed for 4 days against distilled water using a Spectra/Por® dialysis Membrane (cut off used for LPEI 10 kDa=6-8 kDa; cut off used for LPEI 3 kDa/8 kDa=0.5-1 kDa). The FITC-labelled LPEI was lyophilized and stored at -80 °C.

3.11 Formation and evaluation of polyplexes

The amount of LPEI needed for generating polyplexes at a certain N/P ratio was calculated using the following formula (Rodl, 2013):

$$\mu g\ LPEI = \frac{\mu g\ DNA \cdot 43 \cdot N/P\text{-ratio}}{330}$$

43 is the molecular weight of a monomer unit of LPEI and 330 is the mean molecular weight of nucleotides (Rodl, 2013).

Separate solutions of pCMV-Gluc and LPEI (10 kDa) diluted with HBG or HBS to a volume of 5 µl were prepared.

Both solutions were thoroughly mixed for polyplex formation.

Size and ζ-potential of polyplexes were investigated by nanoparticle tracking analysis (NTA) employing NanoSight® NS500 equipped with a 488 nm laser, temperature control, computer controlled motorized stage and focus, sCOMS camera and a manual push/pull filter holder with two fluorescence filters. The device is capable to measure particles of a size between 10 and 2000 nm, in a concentration range between 10^6 to 10^9 particles per ml. For analysis, NTA-software versions 3.0 and 3.1 were used.

The following settings were used for measuring particle size:

Table 4 *NS 500 settings for size measurement*

Number of captures	5
Duration of captures	60 seconds
Temperature	25.0°C

Table 5 *NS500 settings for ζ-potential measurements*

Number of captures	10
Duration of captures	90 seconds
Temperature	25.0°C

As per manufacturer's instructions each sample was diluted to reach a particle concentration between 10 and 100 particles per frame. The tubing system was washed and preloaded with the media used for diluting polyplexes (HBG, RPMI-1640 or HBS) for measurement to avoid differences in the ionic strength within the tubing system.

3.11.1 Polyplexes generated by flash pipetting

Chemicals needed for protocol:

- **Linear polyethylenimine (LPEI) 10 kDa**
- **HEPES buffered glucose (HBG)**
- **pCMV-Gluc**
- **Sodium chloride solution 5 mM**

For polyplex synthesis by flash pipetting 2 µg pCMV-Gluc stock solution was diluted with HBG to 5 µl. The amount of LPEI needed for polyplex formation was calculated using the equation mentioned in chapter 3.11. LPEI was diluted with HBG to a volume of 5 µl. Both solutions were mixed by flash pipetting.

For evaluation of size and ζ-potential of polyplexes generated at different N/P-ratios NanoSight® NS500 was used. After an incubation time of 20 minutes at room temperature the samples were diluted in HBG at a ratio of 1 to 250 for size measurements and 1 to 500 in 5 mM sodium chloride solution for ζ-potential measurements.

Investigations on biophysical properties of polyplexes:

For analyzing the influence of the amount of LPEI used for nanoparticle formation polyplexes were formed at N/P-ratios of 3, 4, 5, 5.5, 6, 7.5, 10, 15 and 30 with a consistent plasmid concentration of 200 µg/ml as described above.

For analyzing the influence pDNA concentration on particle properties polyplexes were generated at pDNA concentrations of 200 µg/ml, 100 µg/ml, 50 µg/ml and 20 µg/ml at N/P 6.

Changes in the properties of polyplexes over time were analyzed using incubation times of 5, 10, 15, 20, 40 and 60 minutes at room temperature.

pDNA concentration after polyplex formation was analyzed by UV spectrophotometry (GE Healthcare NanoVue plus) by using following formula:

$$c\ (pDNA) = (A_{260} - A_{320}) \cdot 50$$

A_{260} gives the pDNA absorption. The background is measured at 320 nm. The result is then multiplied by 50 since (A_{260}-A_{320}) of 1.0 correlates to a DNA concentration of 50µg/ml (https://at.promega.com/resources/pubhub/enotes/how-do-i-determine-the-concentration-yield-and-purity-of-a-dna-sample/, 2015).

3.11.2 Up-scaled Method for the Formation of Polyplexes

Chemicals needed for protocol:

- **Linear polyethylenimine (LPEI) 10 kDa**
- **HEPES buffered glucose (HBG)**
- **HEPES buffered saline (HBS)**
- **RPMI-1640 Medium**
- **pCMV-Gluc**
- **4',6-diamidino-2-phenylindole (DAPI)**
- **Polyplex solution**

A syringe pump (KD scientific, LEGATO 210) was used for an up-scaled, standardized and more reproducible production of polyplexes. The procedure was tested with two different syringe types enlisted in Table 5.

Table 6 *Syringes used for polyplex preparation via syringe pump*

Volume [ml]	***Description***	***Inner diameter [mm]***
1	BBraun Inject F Tuberkulin (Cat.No. 9166017V)	4.74
3	BBraun Omnifix Luerlok Solo (Cat.No. 4617022V)	9.46

The whole procedure was conducted under sterile conditions under a biological safety cabinet.

The syringe pump's construction and functional principle was based on Kasper et al. (Kasper, 2011). We used 3 HPLC tubes connected with a T-connector.

For polyplex formation LPEI containing solution and pDNA containing solution (both dissolved in either HBG or HBS) were soaked into syringes. A dead space of 1 ml was used in each syringe to ensure no loss of product in the tubing system. Then the tubing system was attached. After attaching the syringes into the syringe pump, a flow rate of 1 ml/min was applied while the device was stored vertically. The polyplex solution was collected in a tube. Figure 6 depicts the construction and functional principle of the syringe pump.

Figure 6 *Schematic representation of the syringe pump based system for polyplex generation and functional principle: (1) syringe driver, (2) plunger speed control, (3a) pDNA containing syringe, (3b) LPEI containing syringe, (4) HPLC tubings, (5) T-connector, (6) polyplex, (7) collecting vessel (syringe) (figure from Kasper et al., 2011)*

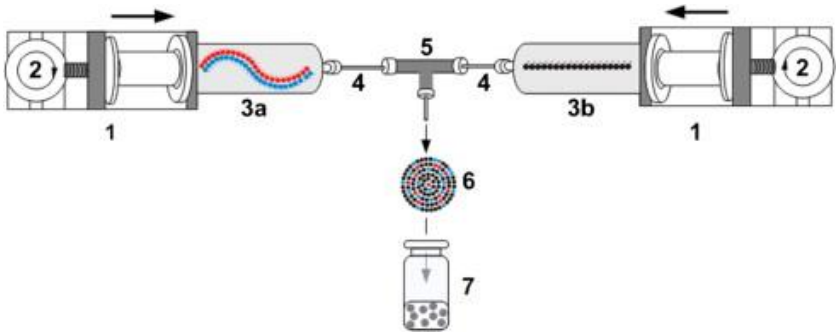

Investigations on biophysical properties of polyplexes:

Size and ζ-potential of polyplexes prepared at N/P-ratio 3, 6 and 9 and a pDNA concentration of 20 µg/ml were generated and prepared for NTA analysis as described in Table 7.

Table 7 *Syringe pump based polyplex formation using HBG/HBS; size and ζ-potential were analyzed using different diluents*

N/P	***generated in***	***diluted in***	***dilution factor***
3	HBG	RPMI-1640	1:10
		HBG	1:50
	HBS	HBS	1:3
6	HBG	RPMI-1640	1:50
		HBG	1:100
	HBS	HBS	1:2
9	HBG	RPMI-1640	1:100
		HBG	1:100
	HBS	HBS	1:2

Investigations on properties of polyplexes with fluorescence microscopy:

Polyplexes generated at a pDNA concentration of 200 µg/ml at N/P 6 diluted in HBG were compared with polyplexes generated at a pDNA concentration of 200 µg/ml at the same N/P-ratio diluted in HBS. Particles were stained with 4',6-diamidino-2-phenylindole (DAPI) using a final DAPI concentration 1 µg/ml. Particles were visualized with an inverted fluorescence microscope (Olympus® IX 71) at 64 x magnification.

4 Results

4.1 Polymer synthesis and characterization

4.1.1 Poly(2-ethyl-2-oxazoline)

Methyl-p-toluenesulfonate was used as initiator for 2-ethyl-2-oxazoline polymerization resulting in with narrow size distribution (Miyamoto, 1988; Chujo, 1990; Miyamoto, 1991; Hochwimmer, 1998; Nuyken, 2002; Lungwitz, 2006).

A representative ^{1}H NMR spectrum of poly (2-ethyl-2-oxazoline) (14 kDa) is depicted in Figure 7.

Figure 7 *^{1}H-NMR of poly(2-ethyl-2-oxazoline): the singlet A (1.09 ppm) corresponds to the methyl protons and the multiplet B (2.24 – 2.37 ppm) to the methylene protons of the propionyl sidechain, the singlet C (3.43 ppm) corresponds to the protons of the polymer backbone's methylene protons. The duplets D (7.12 – 7.17 ppm) and E (7.63 – 7.67 ppm) correspond to the protons of the tosylate counter ion. $CDCl_3$ was used as solvent and internal standard. The shift of the CDCl3 signal was set to 7.26 ppm. The peak in between A and B corresponds to protons of an acetonitrile residue.*

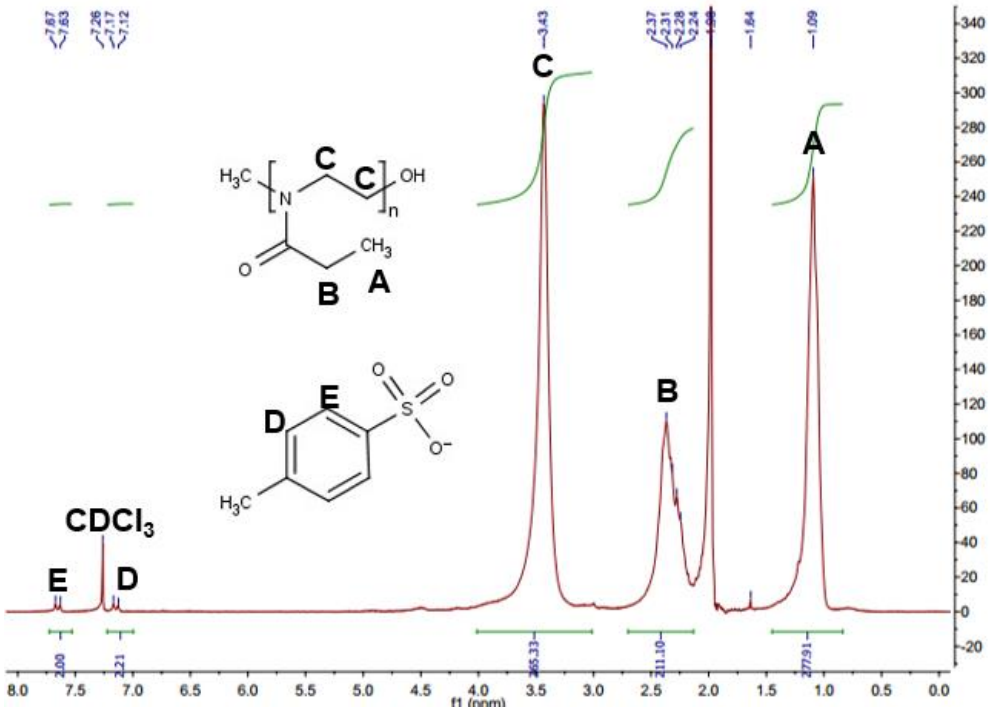

^{1}H-NMR was used to estimate the number average polymerization degree as described by Lungwitz et al. and Brissault et al (Brissault, 2003; Lungwitz, 2006). Therefore the peak area of the aromatic protons of the tosylate counter ion (7.63 and 7.67 ppm) was set to 2 (Figure 12; Signal D and E). The so obtained integrals of the proton signals of the propionyl side chain of the polymer and the methylene backbone of the polymer were used for estimating the M_n of the poly(2-ethyl-2-oxazoline) (Brissault, 2003; Lungwitz, 2006).

However, ^{1}H-NMR analysis only gives approximate values of the molecular weight. Hence, poly(2-ethyl-2-oxazoline) with different degrees of polymerization were analysed by gel permeation chromatography (GPC) which gives number-average (M_n) and mass-average molecular weight (M_w) as well as the polydispersity index (PDI) of the compound (Hoogenboom, 2003). Figure 8 shows the elution profile of poly(2-ethyl-2-oxazoline) of four different molecular weights. The average mass and polydispersity index is enlisted in Table 8. Peaks created at an elution time of >900 seconds correspond to buffer.

Figure 8 *Gel permeation chromatogram of poly (2-ethyl-2-oxazolines) with M_w 6.6, 14.0, 17.0 and 20.0 kDa*

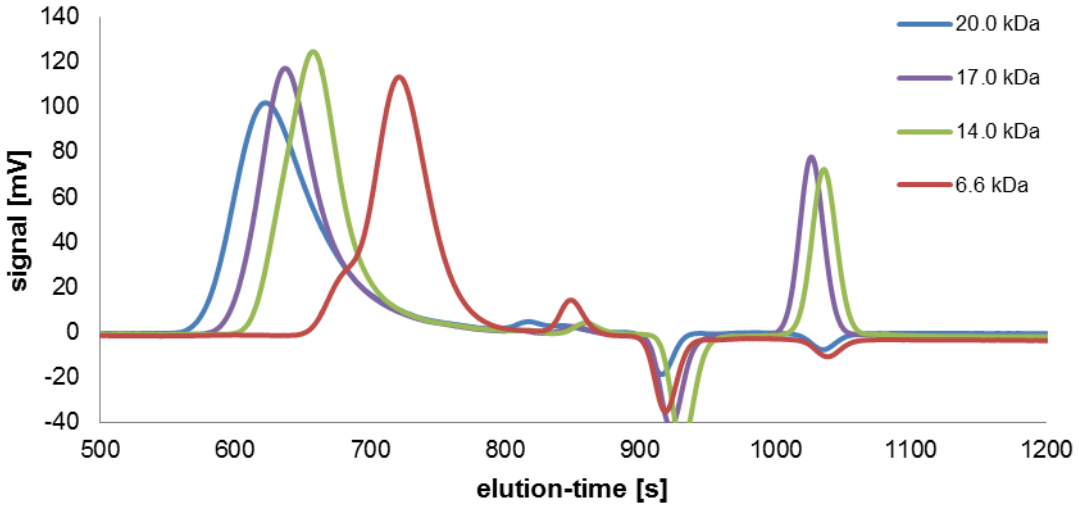

Table 8 *Results of the GPC analysis*

aimed MW [kDa]	M_p [kDa]	M_n [kDa]	M_w [kDa]	PDI [M_w / M_n]
24	22.692	15.706	19.954	1.2705
15	18.832	13.995	17.027	1.2166
10	14.374	11.985	14.004	1.1685
3	6.352	5.937	6.635	1.1176

Side reactions such as proton transfer and chain transfer reactions are possible due to the reactive cationic species finally resulting in polymers characterized by high molecular weight. This was clearly visible in the gel permeation chromatogram of poly (2-ethyl-2-oxazoline) with Mw of 6.6 kDa (Figure 9).

Figure 9 *GP chromatogram of poly(2-ethyl-2-oxazoline) with M_w of 6.6 kDa; a high molecular weight fraction eluted between 650 and 700 seconds, marked by the frame.*

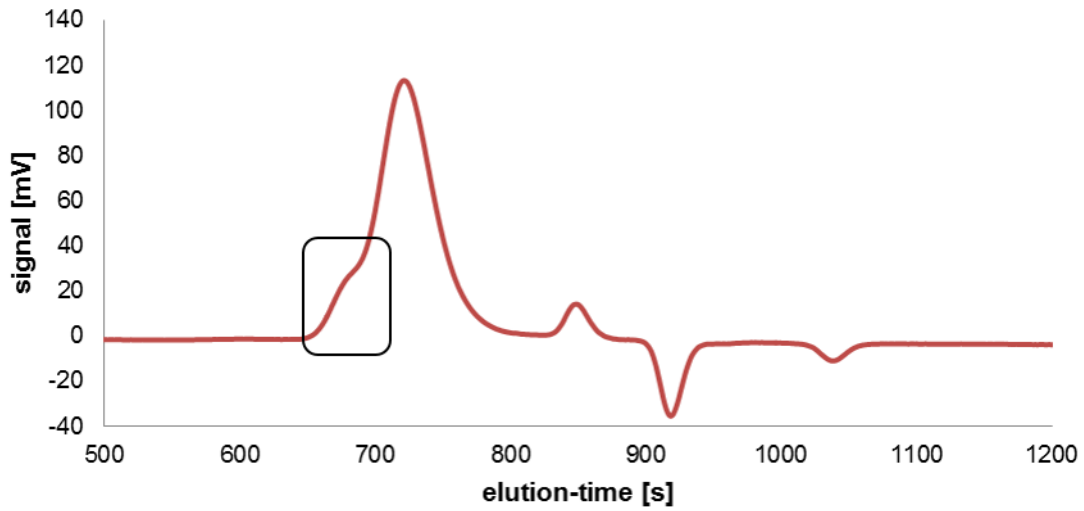

Hence, in process controls by ^{1}H-NMR were done for investigating reaction kinetics during 2-ethyl-2-oxazoline polymerization. ^{1}H-NMR based in process control during the synthesis of poly (2-ethyl-2-oxazoline) with a Mw of 14 kDa is shown as a representative example in Figure 10. 100 % conversion was detected after 21.75 hours.

Figure 10 *Stacked ^{1}H NMR spectra; Measurements were conducted at different time points of the polymerization.*

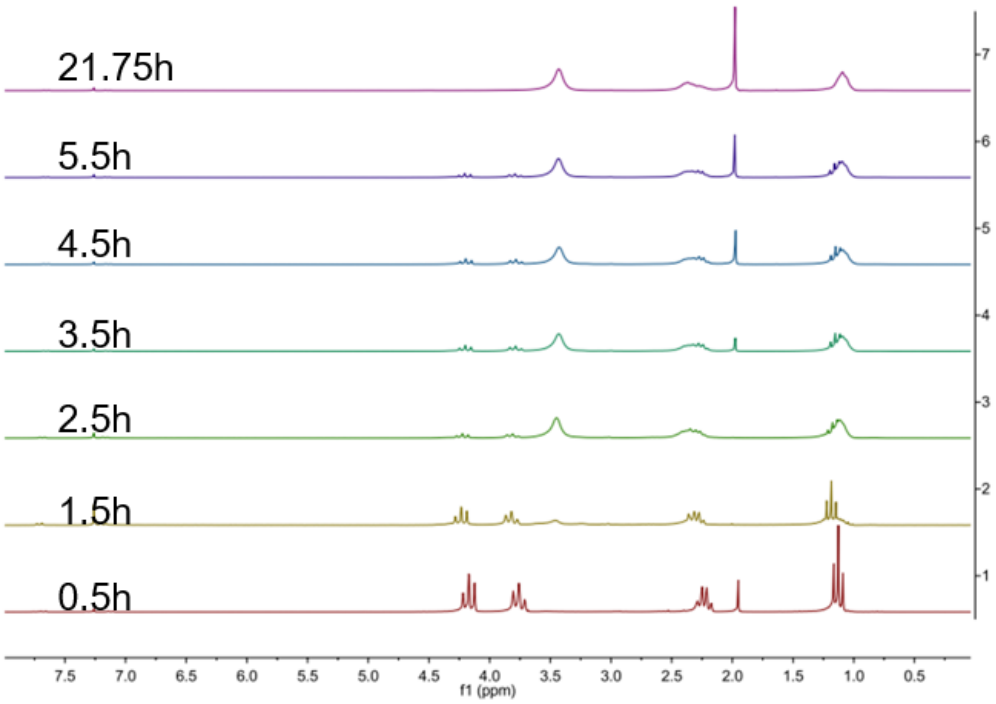

4.1.2 Linear polyethylenimine

Linear polyethylenimine was synthesized according to the protocol of Rödl et al. (Rodl, 2013) by acid hydrolysis of poly (2-ethyl-2-oxazoline) with a Mw of approximately 17 kDa. After alkalizing with 1 M NaOH, LPEI is obtained as free base with an Mw of 6.8 kDa.

The ^{1}H-NMR spectrum of the free base was showing a signal of the proton of the secondary amino group at 1.82 ppm and a signal of the backbone's methylene protons at 2.70 ppm (Figure 11).

Figure 11 *^{1}H-NMR spectrum of LPEI 6.8 kDa; a proton signal of the NH group appeared at 1.82, the signal of the polymer's methylene backbone at 2.70 ppm*

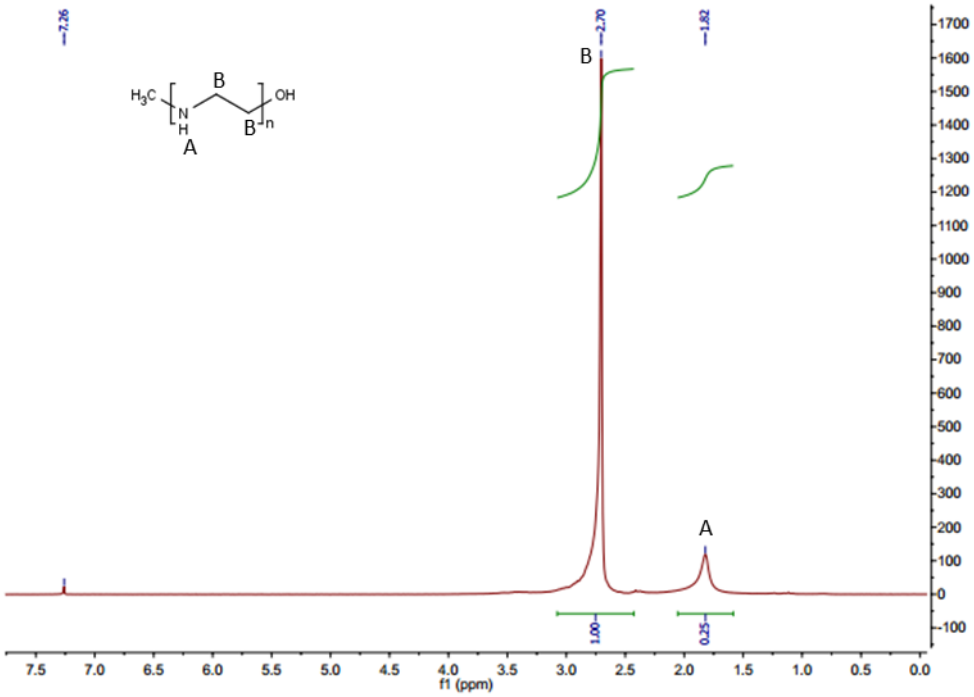

4.2 $LPEI_{10kDa}$-PEG_{2kDa}-cysteine synthesis and characterization

The synthesis of LPEI-PEG-Cys was carried out according to Rödl et al. (Rodl, 2013). L-Cysteine was used instead of the targeting peptide GE11. (Li, 2005; Schafer, 2011)

Synthesis of LPEI (10kDa)-PEG (2 kDa)-OPSS:

LPEI (10 kDa) was conjugated with NHS-PEG (2 kDa)-OPSS linker. For purification, cation exchange chromatography was used. Product containing fractions were eluting at elution volumes between 30 and 50 ml with an increasing NaCl concentration of the eluent and therefore conductivity (Figure 12).

Figure 12 *Cation exchange chromatography profile of LPEI(10kDa)-PEG-OPSS; fractions eluting between 30 and 50 ml were containing the product. The blue line depicts the absorption at 240 nm, the red line at 280 nm, the pink line the absorption at 343 nm. The brown line depicts the NaCl concentration, hence conductivity, of the eluent.*

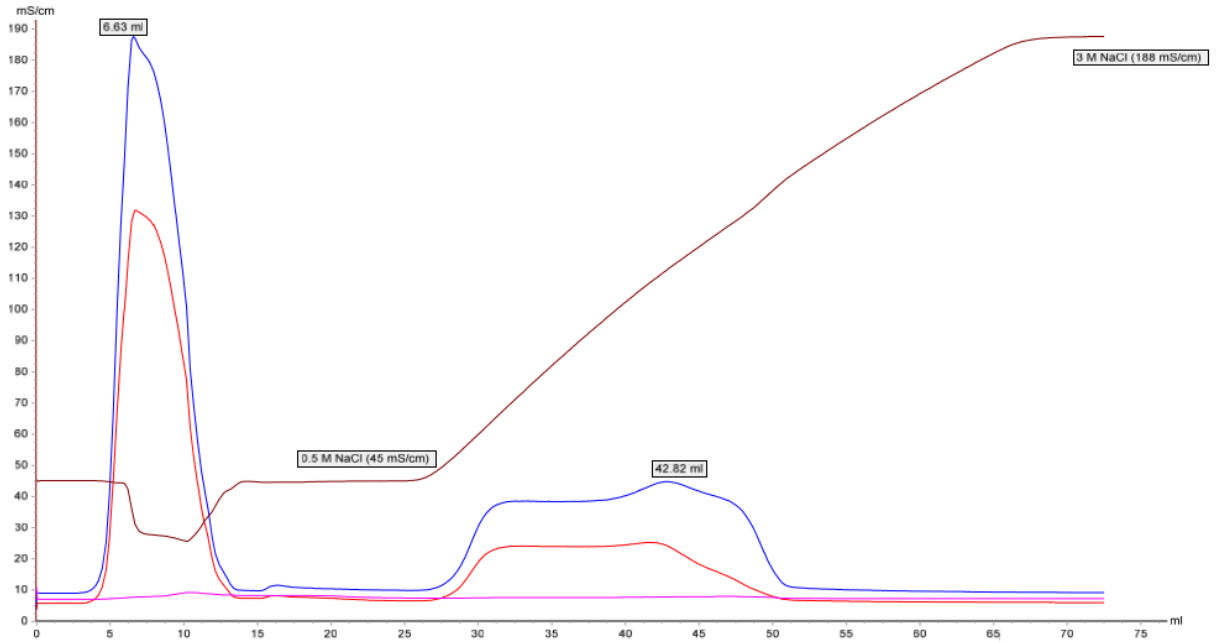

The product was analysed by ^{1}H-NMR using D_2O as solvent. The spectrum is characterized by a signal at 2.95 ppm corresponding to the protons of LPEI and a signal at 3.63 ppm, corresponding to the protons of PEG (Figure 13).

The ratio of between PEG and LPEI in the conjugate was determined by ^{1}H NMR.

Figure 13 *^{1}H-NMR spectrum of LPEI-PEG-OPSS*

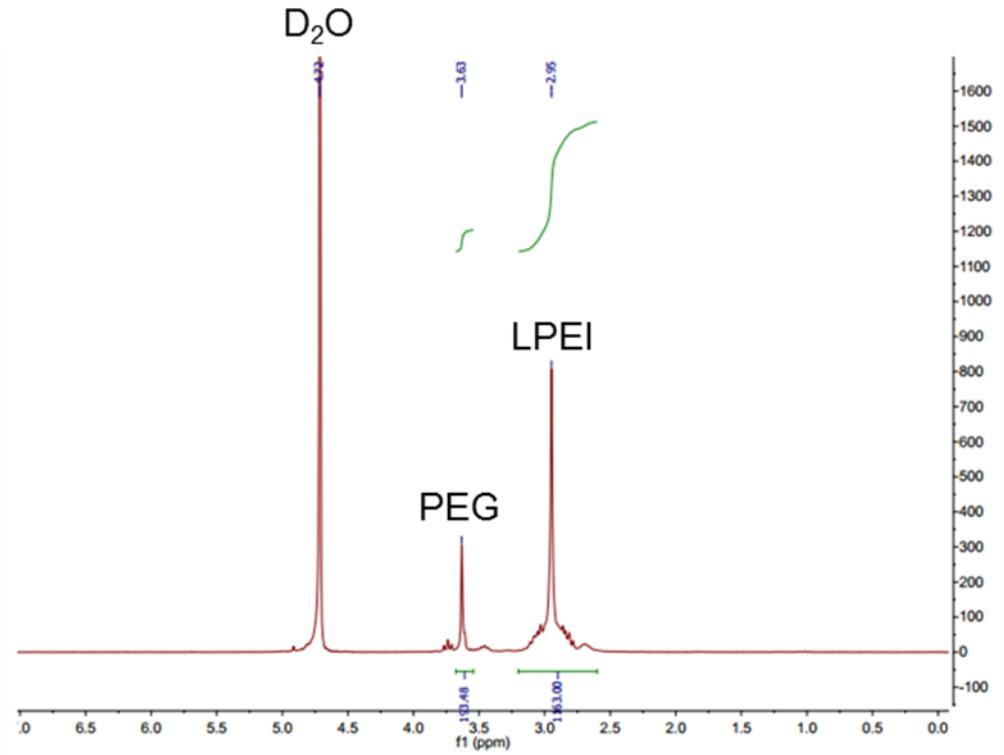

The LPEI signal was used for normalizing the PEG signal.

$$\frac{10\ 000}{43} \cdot 5 \cong 1163 \text{ H of LPEI } (_{10kDa})$$

10,000 is the weight average molecular weight of LPEI. 43 the molecular weight of one LPEI subunit. The ratio between those two values gives the number of monomer subunits in the polymer. This multiplied by 5 which is the amount of protons per monomer gives the total amount of protons in the polymer. The LPEI signal was therefore normalized to 1,163. The integral of the PEG signal was used for calculating the average number of PEG molecules per LPEI molecule.

The total amount of protons in the PEG molecule was calculated as follows:

$$\frac{2\,000}{44} \cdot 4 \cong 182 \text{ H of PEG}$$

2,000 is the molecular weight of PEG, 44 the molecular weight of one subunit and 4 the number of protons per subunit.

The molar ratio between PEG and LPEI was calculated by dividing the integral value of the PEG signal by the total amount of protons per PEG molecule.

$$\frac{194}{182} \cong 1{,}07 \text{ molecules PEG per molecule } LPEI_{10kDa}$$

Synthesis of LPEI (10kDa)-PEG (2 kDa)-cysteine

Cysteine was used in a 2-fold molar excess corresponding to PEG-OPSS. The progress of the reaction was observed via UV-spectroscopy whereby the absorption of released thiopyridone was measured at 343 nm. The reaction was complete after 60 minutes as the absorption wasn't increasing anymore (Table 9).

Table 9 *Absorption of thiopyridone at 343nm at different time points*

Time [minutes]	A_{343nm}
0	1.095
30	1.117
60	1.158
90	1.156
120	1.155
150	1.154

After full conversion, the product was purified by cation exchange chromatography as described in chapter 3.9. With an increasing NaCl concentration in the eluent and therefore conductivity, the product containing fractions eluted between 40 and 45 ml elution volume (Figure 14).

Figure 14 *Cation exchange chromatography profile of LPEI (10kDa)-PEG (2kDa)-Cys; fractions eluting between 40 and 45 ml contained the product. The blue line depicts the absorption at 240 nm, the red line at 280 nm, the pink line the absorption at 343 nm. The brown line depicts the NaCl concentration, hence conductivity, of the eluent.*

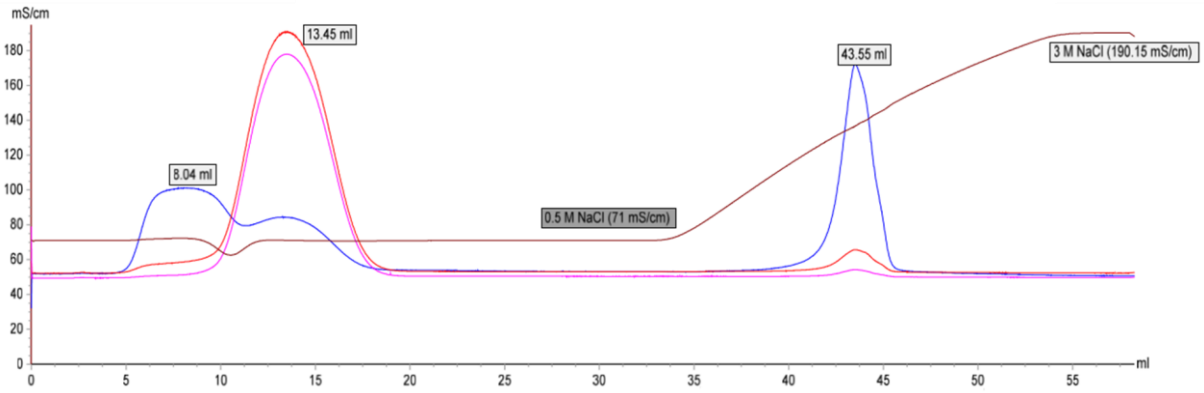

4.3 Evaluation of Plasmid/LPEI Polyplexes

The influence of various parameters like different N/P-ratios, pDNA concentrations, incubation times and diluents on biophysical properties of polyplexes were investigated. Additionally an up-scaled polyplexing method utilizing a syringe pump was optimized.

All samples were analysed by NTA giving high resolution measurements (Filipe, 2010).

Additionally to NTA measurements pDNA recovery after polyplex formation was determined by UV spectrophotometry to prove the stability of nanoparticles.

4.3.1 Influence of N/P-ratio on nanoparticle properties

Polyplexes were prepared in HBG at N/P-ratios of 3, 4, 5, 5.5, 6, 7.5, 10, 15 and 30 at a constant pDNA concentration of 200 µg/ml which is commonly used for *in vivo* experiments and analysed by NTA (Schafer, 2011).

Figure 15 *Outcome of NTA measurements of polyplexes generated at different N/P-ratios at a constant plasmid concentration of 200 µg/ml. Grey bars depict the mean values of size of nanoparticles (y-axis). Black squares depict the mean values of the standard deviations of the NTA measurements. (n = 3, values are depicted as mean +/- s.d.)*

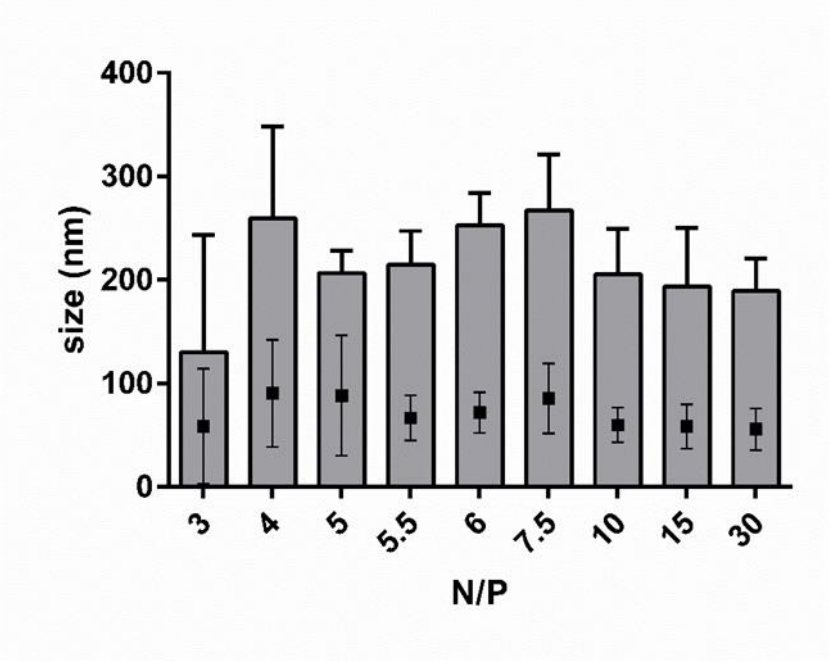

NTA size determinations revealed, that particles are getting smaller from N/P 10 upwards. Polyplexes with an N/P ratio of 3 had a significantly higher standard deviation compared to polyplexes generated at higher N/P ratios. This is due to instability of the particles at this low ratios, leading to aggregation. Most of this aggregates then precipitateand cannot be detected by NTA, leading to low registered particle concentration and broad size distribution of the measured sample.

The samples with N/P-ratios of 6 and 7.5 seem to be outliners, at least it cannot be explained yet why they were significantly bigger than polyplexes generated at N/P ratios 5 and 5.5. This also resulted in a markedly lower percentage in the size range between 100 and 200 nm of the two representatives.

However, the overall outcome of the NTA measurements showed, by increasing the N/P-ratio the tendency of polyplexes is to become smaller (Figure 15). With an increasing N/P ratio the percentage of particles with a size between 100 and 200 nm gets bigger (Figure 16). Based on previous publications the percentage of particles with a size between 100 and 200 nm directly correlates with the transfection efficiency *in vivo* (Wightman, 2001). ζ-potential increases with the N/P ratio (Figure 17).

Figure 16 *Percentage of particles in the size range between 100 and 200 nm (y-axis), correlating to the N/P-ratios of the polyplexes (x-axis). (n = 3, values are depicted as mean +/- s.d.)*

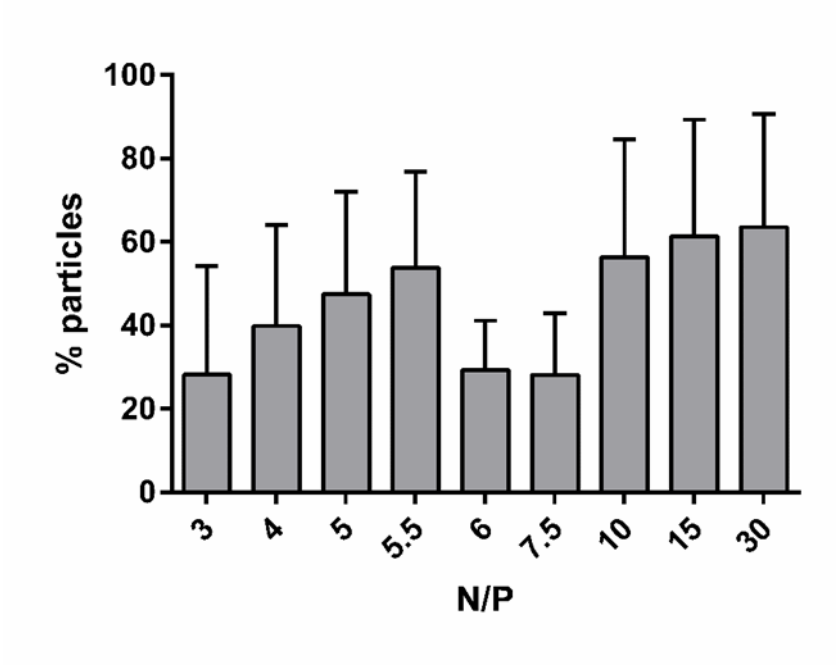

Figure 17 *NTA based ζ-potential measurements of polyplexes generated at different N/P-ratios at a constant plasmid concentration of 200 µg/ml. The plot depicts the zeta potential of the particles (y-axis), correlating to the N/P-ratios of the polyplexes (x-axis). (n = 3, values are depicted as mean +/- s.d.)*

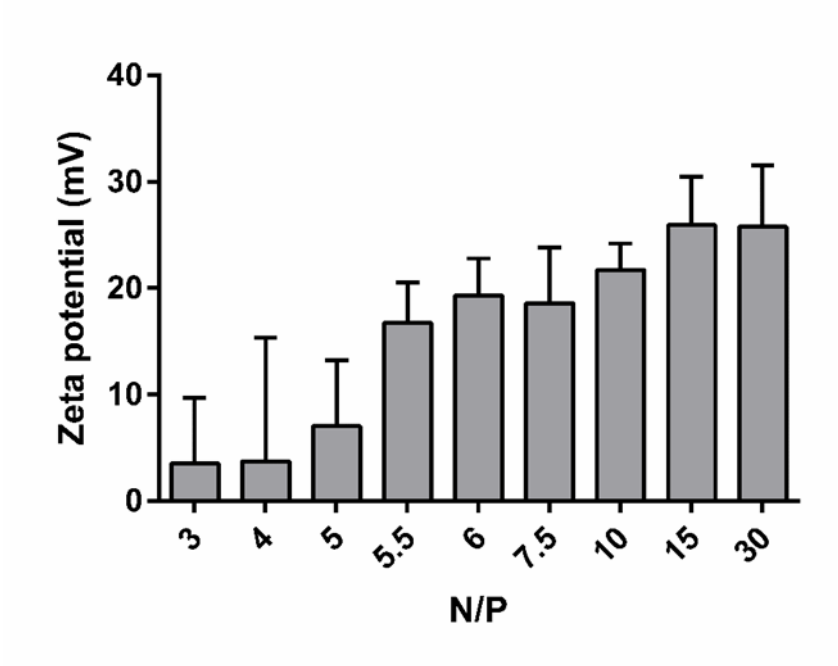

Polyplexes generated at N/P ratios from 3 to 5 showed a high polydispersity which is shown by averaging the individual standard deviations of the size measurements, calculated by the NTA software. Especially polyplexes prepared at N/P 3 have low kinetic stability and tend to aggregate more compared to polyplexes prepared at higher N/P-ratios. This was investigated by NTA and by measuring pDNA recovery. Therefore, the pDNA concentration of the polyplex solution was determined by Nanodrop UV spectrophotometer and compared with the pDNA concentration of 200 µg/ml which was used for polyplexing. There it is clearly visible that especially at an N/P-ratio of 3 approximately 50 % of the initially used amount of plasmid precipitated (approximately 100 µg/ml vs. 200 µg/ml pDNA concentration of the tested solution, Figure 18)

Two representative NTA derived size plots of polyplexes with an N/P 3 and 30 are compared and illustrate the significant difference in size distribution. While polyplexes with an N/P-ratio of 3 are showing a wide range of size distribution, polyplexes with an N/P-ratio of 30 are distributed significantly narrower (Figure 19).

Figure 18 *Nanodrop determinations of the plasmid recovery of the polyplexes formed at different N/P-ratios. Especially polyplexes with an N/P-ratio of 3 tend to aggregation and often precipitated. (n = 3, values are depicted as mean +/- s.d.)*

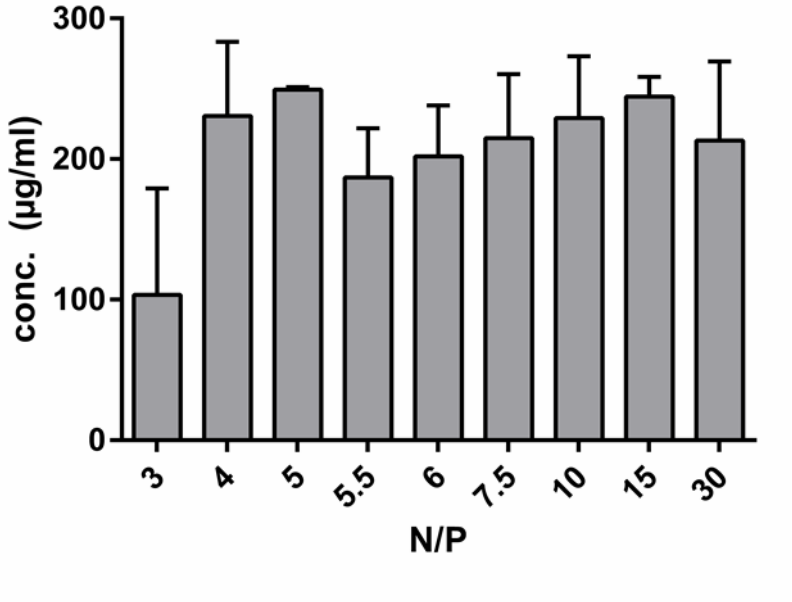

Figure 19 *Comparison of the NTA plots of polyplexes with an N/P-ratio of 3 (left) and 30 (right). The difference in size distribution can be clearly observed: while polyplexes with an N/P-ratio of 3 show a wide range of size distribution, the polyplexes with an N/P-ratio of 30 are distributed significantly narrower.*

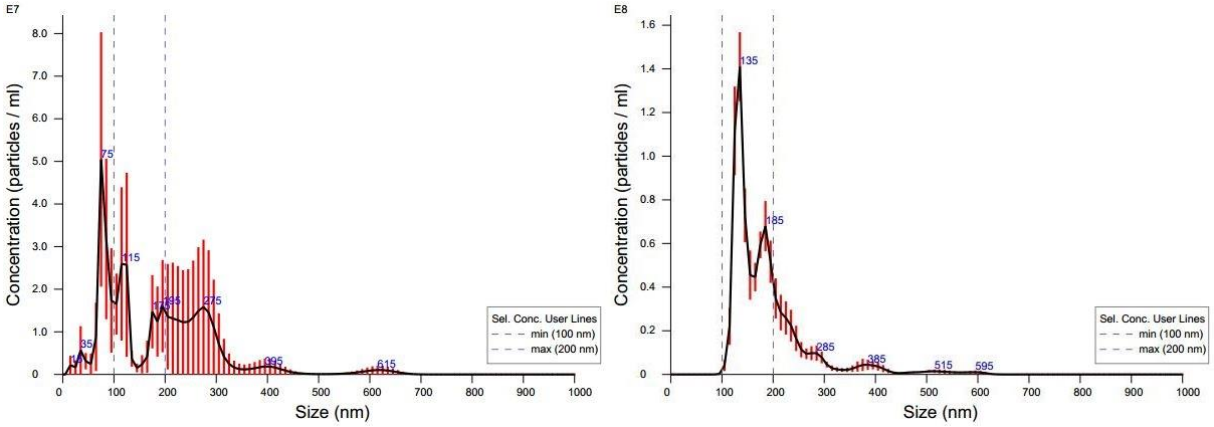

4.3.2 Influence of pDNA concentration on nanoparticle properties

For investigating the influence of pDNA concentration on polyplex properties particles were generated in HBG at a constant N/P-ratio of 6 at pDNA concentrations of 20, 50, 100 and 200 µg/ml.

The particle size increased with pDNA concentration (Figure 20) in accordance to literature (Kasper, 2011). The percentage of particles in a range between 100 and 200 nm showed the highest value at polyplexes generated with a pDNA concentration of 50 µg/ml (Figure 21).

Investigation of pDNA recovery revealed no significant precipitation after particles were generated.

This enhanced aggregation behaviour of polyplexes at higher pDNA concentrations correlates well to the literature (Fernandez, 2009; Kasper, 2011).

Figure 20 *Outcome of NTA measurements of polyplexes generated at different pDNA concentrations at a constant N/P-ratio of 6. Grey bars depict the mean values of size of the polyplexes (y-axis) correlating to the individual pDNA concentration (x-axis). Black squares depict the mean values of the individual standard deviations of each NTA measurement. (n = 2, values are depicted as mean +/- s.d.)*

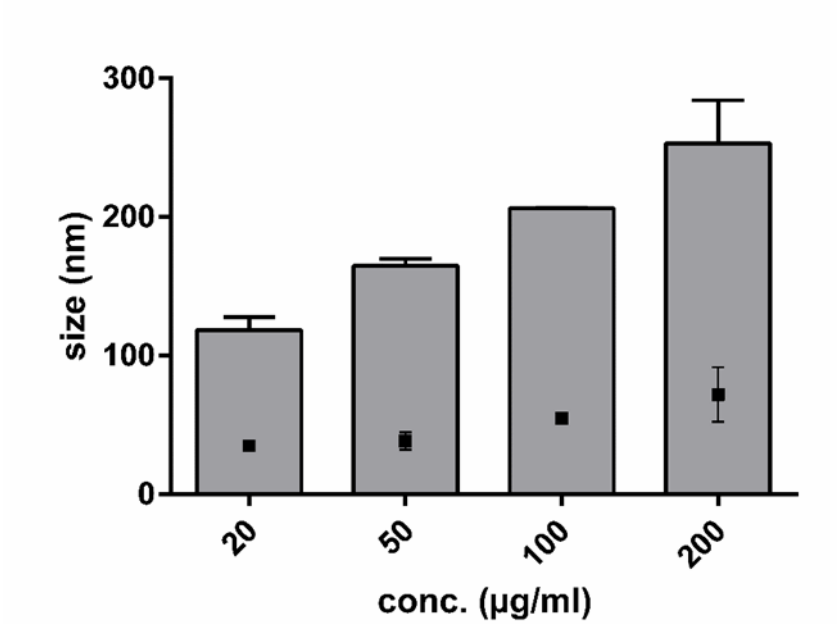

Figure 21 *NTA measurements of polyplexes generated at plasmid concentrations at a constant N/P-ratio of 6. The plot depicts the percentage of particles in the range between 100 and 200 nm (y-axis), correlating to the pDNA concentration of the polyplexe solution (x-axis). (n = 2, values are depicted as mean +/- s.d.)*

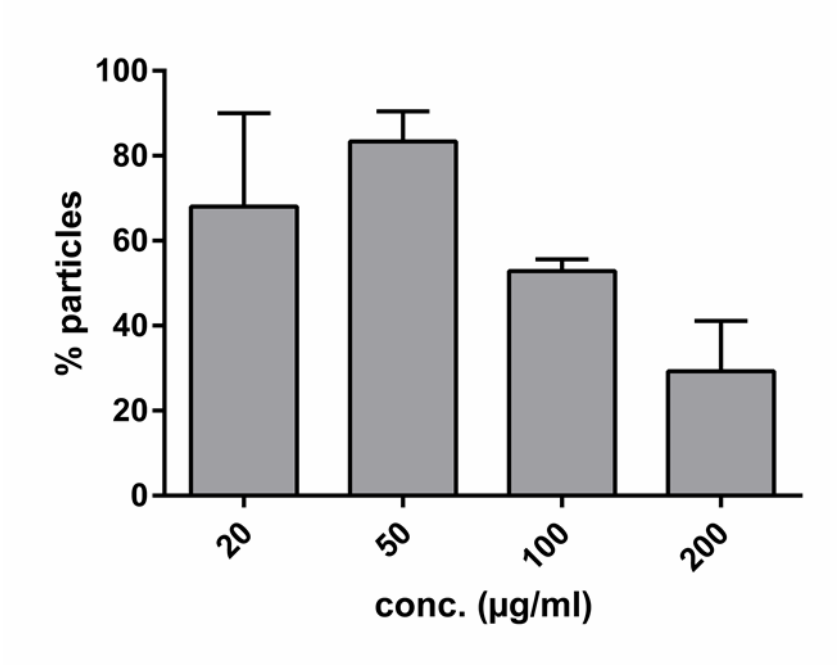

4.3.3 Influence of incubation time on nanoparticle properties

For investigating the influence of incubation time on particle size a polyplex solution was made with an N/P ratio of 6 and a pDNA concentration of 200 µg/ml. NTA measurements were then carried out 0, 5, 10, 15, 20, 40 and 60 minutes after polyplex generation.

After an increase in the particle size during the first 20 minutes the particle size became smaller again (Figure 22). The reason could be explained by precipitation of particles starting after 20 minutes. Due to their big size the so obtained aggregates could not be detected by NTA making the average size and standard deviations of the detected particles smaller.

Figure 22 *Outcome of NTA measurements of polyplexes in an incubation timeline from 0 to 60 minutes. The plot depicts the average size of particles (y-axis) at different time points (x-axis). (n = 2, values are depicted as mean +/- s.d.)*

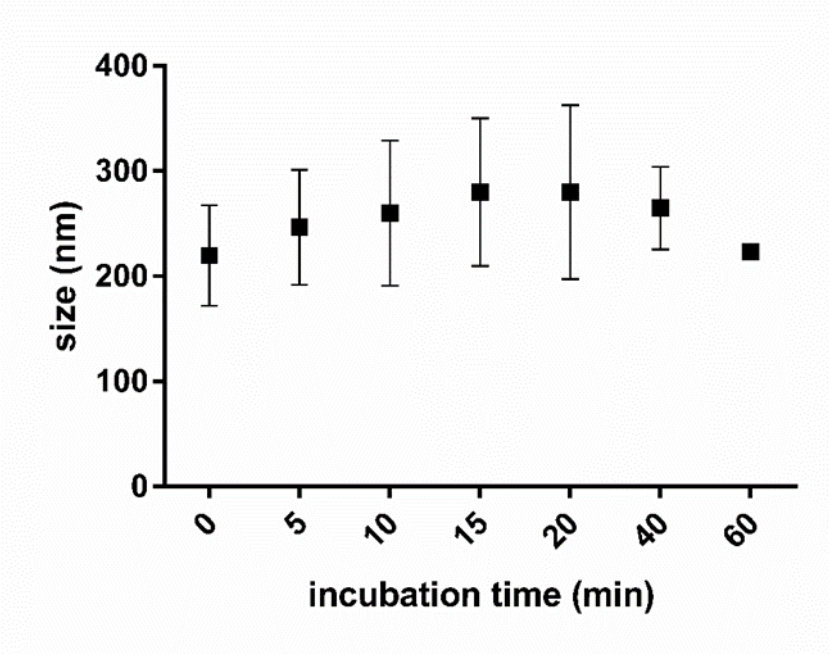

4.3.4 Optimization of an up-scaled method for synthesizing polyplexes

Due to batch-to-batch variability and the limitation to low volumes of polyplex generation by flash pipetting we optimized an up-scaled, more reproducible synthesis method for generating polyplexes by using a syringe pump which was described by Kasper et al. (Kasper, 2011).

Regarding biophysical properties there was no significant difference between 1 ml and 3 ml syringes of BBraun. For further experiments we always used 3 ml BBraun Omnifix syringes for polyplex generation because a volume of 1 ml is insufficient when it comes to upscaling.

We chose a flow rate of 1.0 ml/min resulting in particles with the lowest polydispersity and highest percentage in a size range between 100 and 200 nm, compared to flow rates of 0.1 and 0.5 ml/min (Figure 23). This result was well according to the findings of Kasper et al. who found a decrease of average size and polydispersity when increasing the flowrate (Kasper, 2011).

Figure 23 *NTA based results of polyplexes made at flow rates of 0.1, 0.5 and 1.0 ml/min with a 3 ml syringe – average diameter is compared in the left plot, percentage of particles in a size range between 100 and200 nm in the left plot. (n = 2, values are depicted as mean +/- s.d.)*

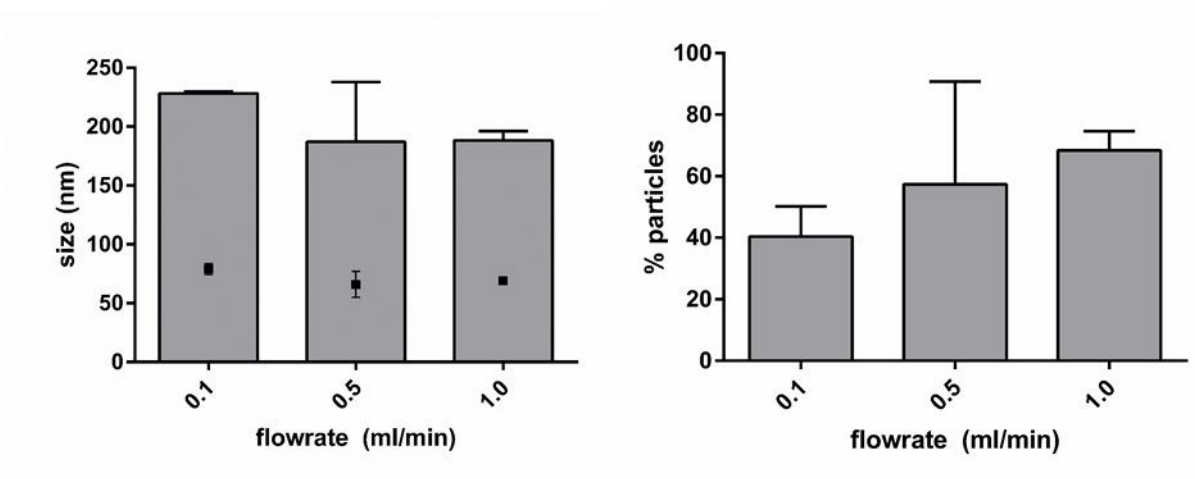

The size of polyplexes made by this syringe pump based method was compared with the size of polyplexes made by flash pipetting of 3 different users via NTA. Thereby we wanted to show the user dependence of the flash pipetting technique.

The analysis showed that polyplexes made by flash pipetting and polyplexes made by syringe pump based synthesis are in approximately the same size range (Figure 24). However, the advantage of the syringe pump method is the possibility to generate reproducible polyplex batches of greater amounts which is limited with the classic flash pipetting method.

Figure 24 *NTA based size measurements of polyplexes (HBG used as buffer, N/P 6, plasmid concentration of 20 µg/ml) made by pipetting of 3 different users compared to polyplexes made via syringe pump. (n = 3, values are depicted as mean +/- s.d.)*

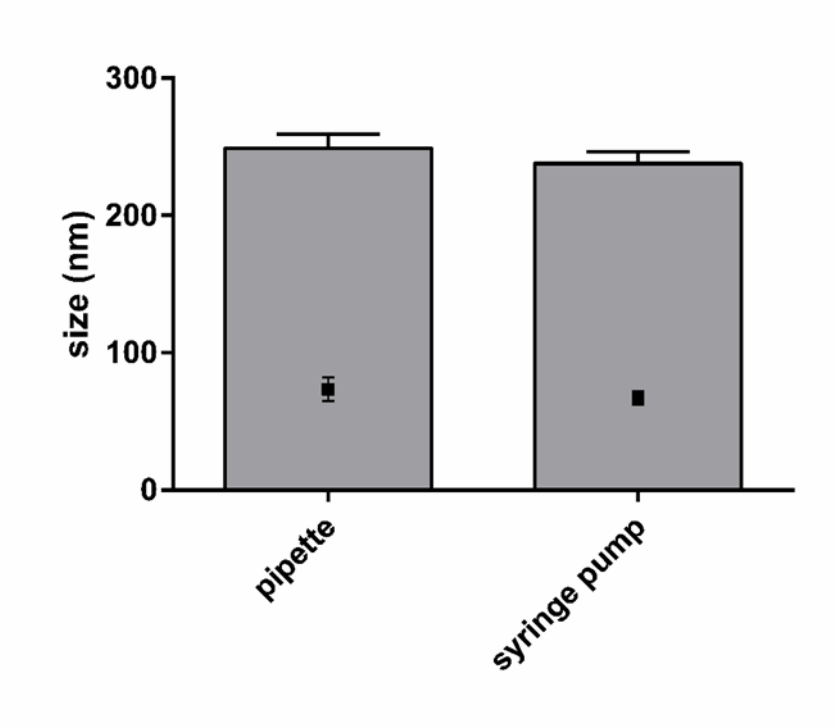

4.3.5 Influence of media

The influence different diluents (HBG, RPMI 1640) on the particle size was investigated by NTA. Polyplexes were generated in HBG at N/P-ratio 3, 6 and 9 and a pDNA concentration of 20 µg/ml.

Diluting the sample in RPMI 1640 enables the simulation of changes in the particle size which occur during *in vitro* testing.

Figure 25 *NTA measurements of polyplexes diluted in HBG or RPMI 1640. The light grey bars depict the size of particles diluted in HBG, the dark grey bars the size of particles diluted in RPMI 1640. The black squares depict the mean values of the standard deviations of the individual measurements. (n = 3, values are depicted as mean +/- s.d.)*

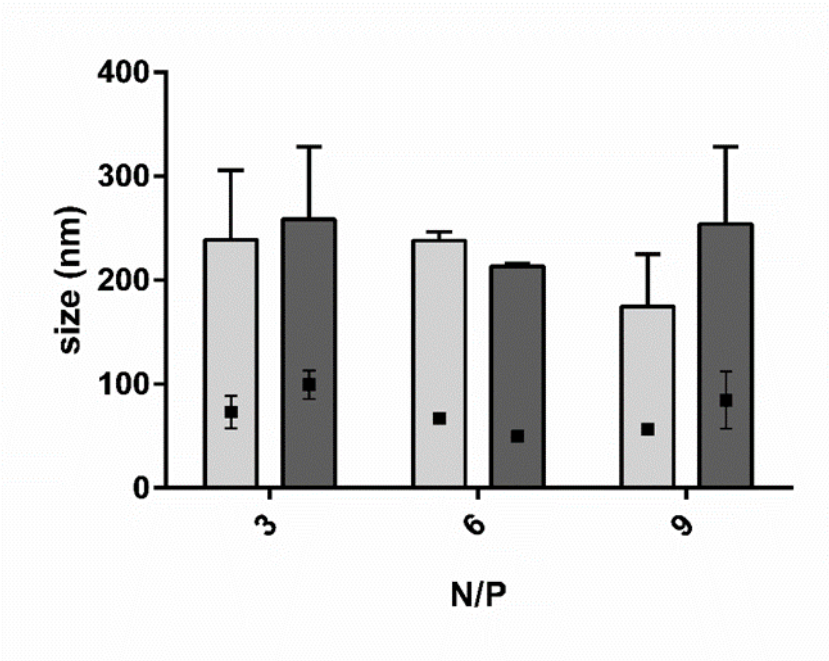

The results of the NTA measurements show that RPMI 1640 has an influence on average diameter of polyplexes. For example, polyplexes prepared at N/P-ratio 9 showed a mean size which was significantly bigger when diluted in RPMI 1640 (Figure 25).

Also the percentage of particles with a size between 100 and 200 nm was significantly lower when diluted with RPMI 1640 instead of HBG especially at N/P-ratios of 3 and 9 (Figure 26).

Figure 26 *NTA measurements of polyplexes with N/P-ratios of 3, 6 and 9 diluted in HBG (light grey bars) or RPMI 1640 (dark grey bars). The plot depicts the percentage of particles in the range between 100 and 200 nm (y-axis), correlating to the plasmid concentrations of the polyplexes (x-axis). (n = 3, values are depicted as mean +/- s.d.)*

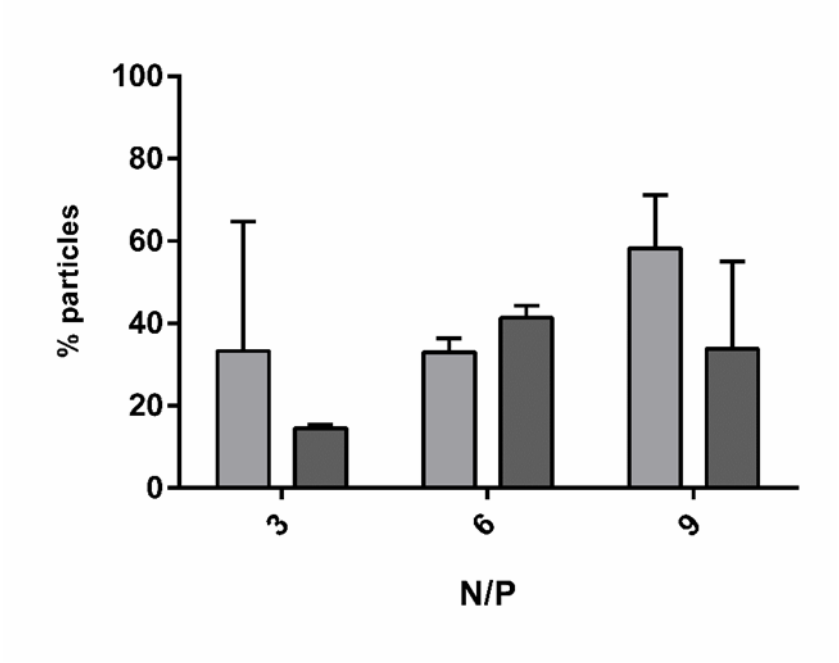

4.3.6 Influence of buffer system on polyplex properties

For evaluating the influence of the synthesis buffer on particle properties polyplexes were generated in HBS at N/P-ratio 3, 6 and 9 with a plasmid concentration of 200 µg/ml. HBS was used as a diluent for NTA measurements. Strong aggregation of particles was observed (Figure 27).

Particles prepared at pDNA concentrations of 200 µg/ml showed significant precipitation which made NTA analysis impossible (Figure 28).

The aggregation tendency of particles prepared in HBS was analysed by fluorescence microscopy. Therefore, particles at N/P 6 and a pDNA concentration of 200 µg/ml were prepared in HBG and HBS, respectively. After an incubation time of 20 minutes particles were stained with DAPI and visualized by fluorescence microscopy.

Figure 27 *Fluorescence microscopy pictures of (A) DAPI stained polyplexes generated in HBG (plasmid concentration 200 µg/ml; incubation time 20 minutes) and (B) DAPI stained polyplexes generated in HBS (plasmid concentration 200 µg/ml; incubation time 20 minutes).*

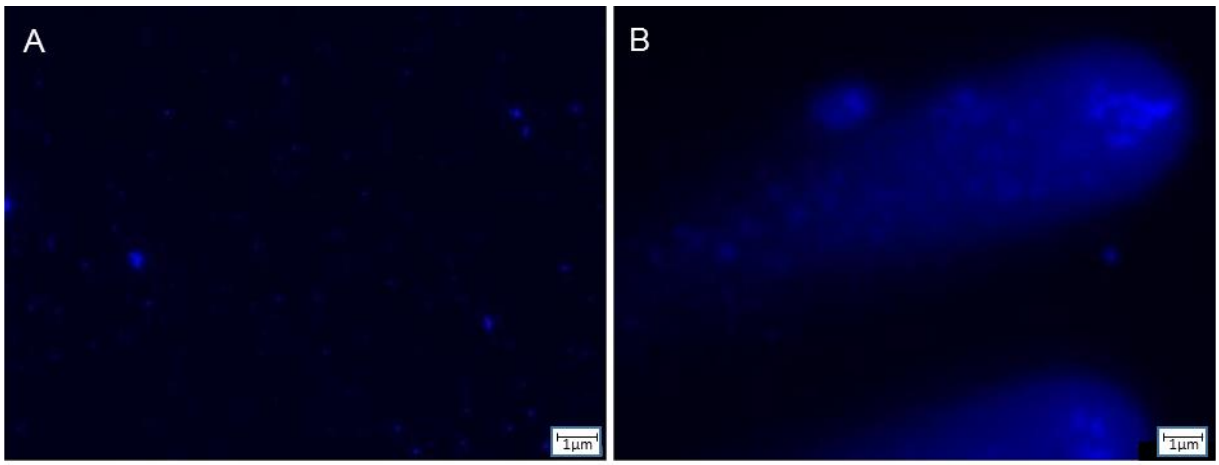

While polyplexes formed in salt free HBG with a pDNA concentration of 200 µg/ml remained rather small polyplexes generated in HBS formed markedly big aggregates (Figure 27).

Figure 28 *NTA measurements of polyplexes formed and diluted in HBS and HBG respectively. The light grey bars depict the size of particles generated and diluted in HBG, the dark grey bars the size of particles generated and diluted in HBS. The black squares depict the mean values of the individual standard deviations of the individual measurements. (n = 3, values are depicted as mean +/- s.d.)*

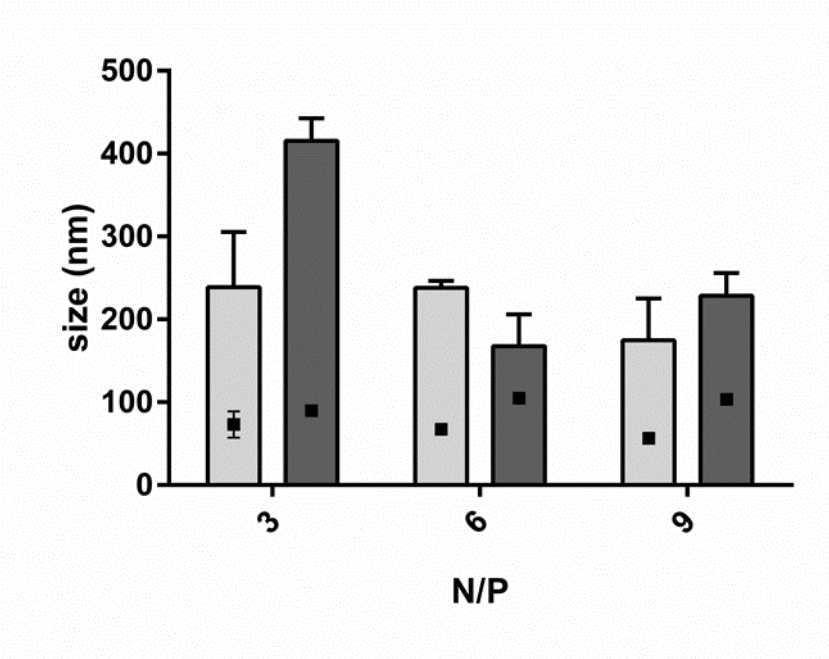

NTA measurements of particles prepared in HBS at a pDNA concentration of 20 µg/ml show that especially at N/P 3 the particles have a markedly bigger average diameter (415.5 nm) than polyplexes generated and diluted in HBG (239.0 nm) (Figure 28).

So it is not surprising that the percentage of particles in a range of 100 to 200 nm were significantly higher of polyplexes formed and diluted in HBG than of those formed and diluted in HBS (Figure 29).

This aggregation behaviour of polyplexes generated in HBS was the reason why lower dilution factors (1:2 or 1:3, respectively) were needed to obtain an appropriate concentration of particles for NTA measurements, compared to polyplex solutions generated in HBG, where dilution factors of 1:10, 1:50 or 1:100 (depending on N/P-ratio) were needed (see Table 7, page 32).

Figure 29 *NTA measurements of polyplexes with N/P-ratios of 3, 6 and 9 generated and diluted in HBG (light grey bars) and HBS (dark grey bars) respectively. The plot depicts the percentage of particles in the range between 100 and 200 nm (y-axis), correlating to the plasmid concentrations of the polyplexes (x-axis). (n = 3, values are depicted as mean +/- s.d.)*

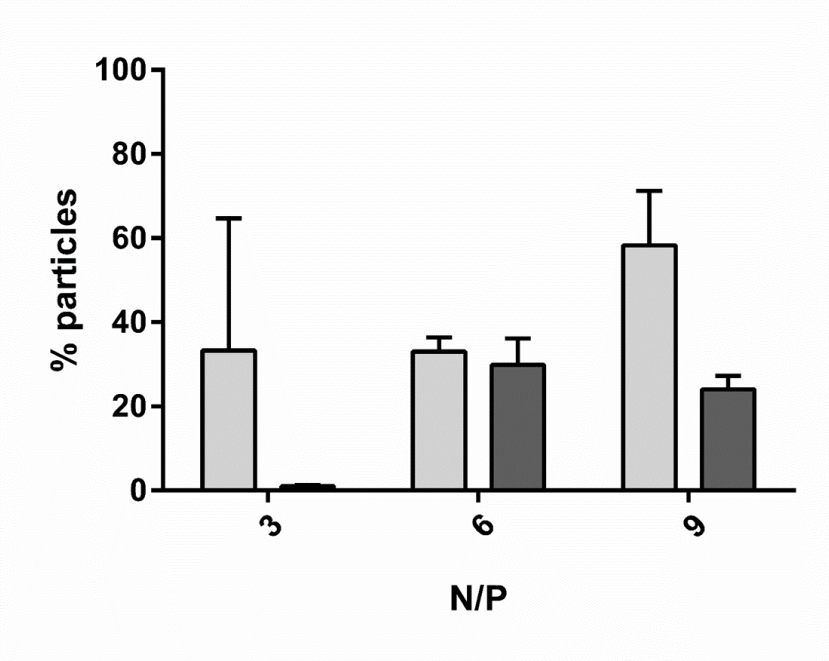

Determination of pDNA recovery revealed that no significant amount of polyplexes precipitated after their generation. The ratio between concentrations of pDNA before and after polyplexing was approximately 1.0 in all measurements (Figure 30).

Figure 30 *pDNA recovery of polyplexes made in HBG (light grey bars) and HBS (dark grey bars) (n = 3, values are depicted as mean +/- s.d.)*

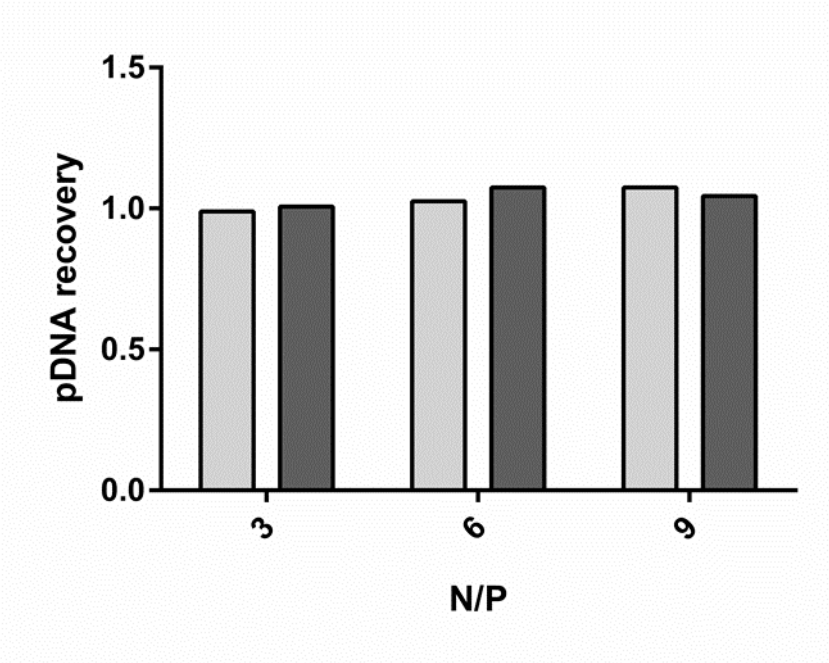

4.4 Fluorescent labelling of LPEI

We attempted to stain LPEI with Fluorescein 5(6)-isothiocyanate (FITC) and observed the fluorescent emission of polyplexes generated with LPEI-FITC with NS500. Emission fainted rather quickly after exposure to the laser. Hence, no results could be obtained.

5 Discussion

5.1 Polymer synthesis and characterization

In this thesis we worked on optimizing a synthesis of poly(2-ethyl-2-oxazoline) which can be used as precursor for LPEI synthesis. For this purpose cationic ring-opening polymerization of 2-ethyl-2-oxazoline was carried out as described in literature (Schaffert, 2013).

We chose methyl-p-toluenesulfonate as initiator for this polymerization, as it is shown that resulting poly(2-ethyl-2-oxazolines) exhibits narrow size distribution (Miyamoto, 1988; Chujo, 1990; Miyamoto, 1991; Hochwimmer, 1998; Nuyken, 2002; Lungwitz, 2006).

Figure 31 shows the mechanism of initiation and propagation of the reaction.

Figure 31 *Reaction Scheme of (a) initiation and (b) propagation of the polymerization of 2-ethyl-2-oxazoline with the poly(2-ethyl-2-oxazoline) as final product.*

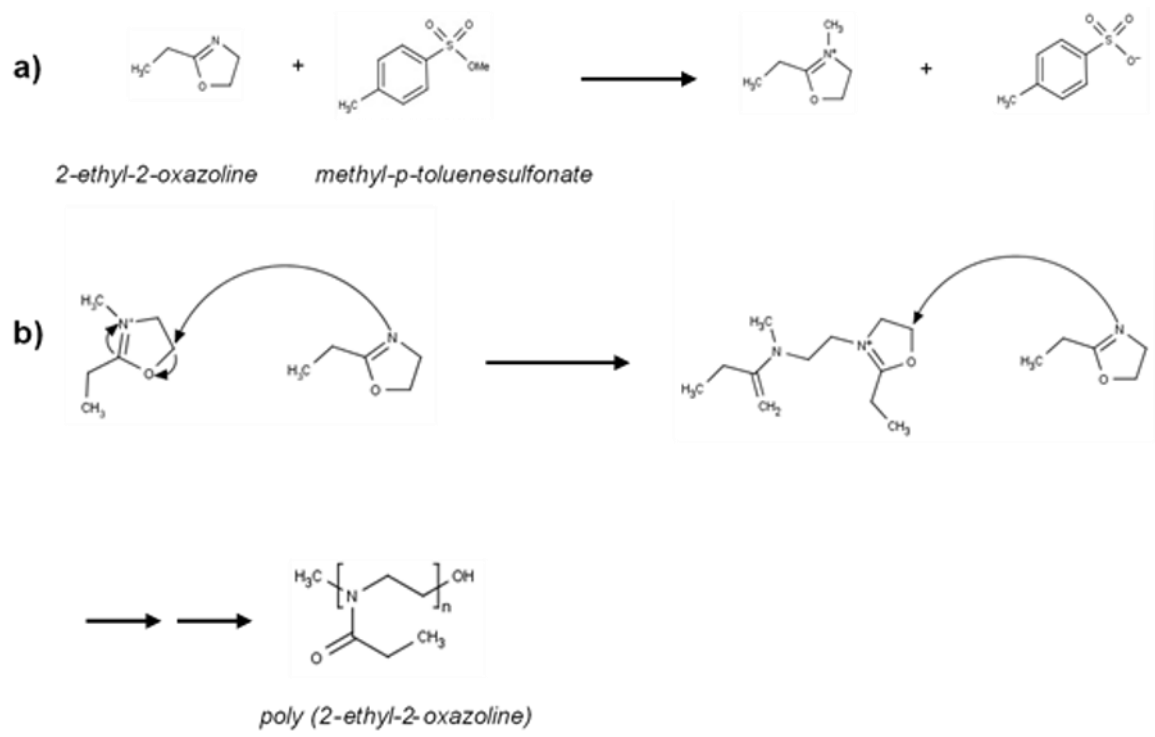

GPC showed the receipt of poly(2-ethyl-2-oxazoline) with M_W between approximately 6.635 and 19.954 kDa and polydispersity indexes between approximately 1.1 and 1.3. Polyethylenglycol was used as a standard for GPC measurements. The polydispersity increased with the degree of polymerization. It also revealed that the theoretical molecular weights of the poly(2-ethyl-2-oxazolines) with 10 and 15 kDa are approximately concurring with the results, while the 3 and the 24 kDa poly (2-ethyl-2-oxazolines) showed bigger deviations.

When the reaction is carried out too long formation of hindered enamines proton transfer and chain transfer reactions resulting in high molecular weight side products is possible (Figure 32) (Litt, 1975). Hence, we carried out in-process controls by ^{1}H-NMR for determining the endpoint of polymerization. In case of poly(2-ethyl-2-oxazoline) with M_w of 14 kDa reaction kinetics showed complete conversion after 21.75 hours.

Figure 32 *Chain end transfer reaction of poly(2-ethyl-oxazoline)*

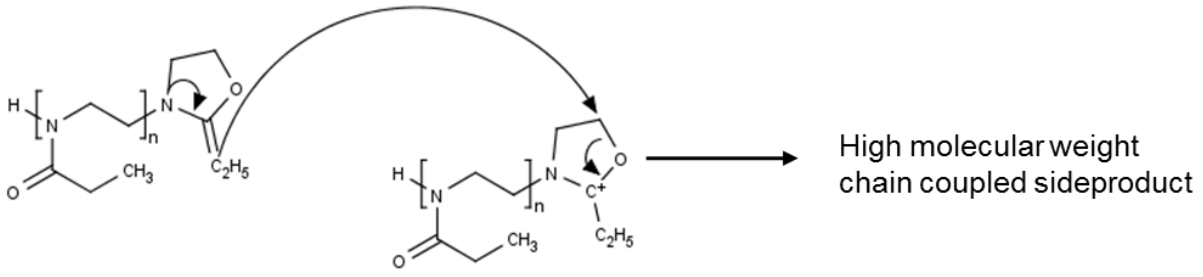

Poly(2-ethyl-2-oxazoline) with M_w of 17 kDa was used for synthesizing LPEI with M_w of 7.4 kDa by acidic hydrolysis after the protocol of Rödl et al. (reaction mechanism depicted in Figure 33) (Rödl, 2013).

Figure 33 *Reaction mechanism of LPEI synthesis*

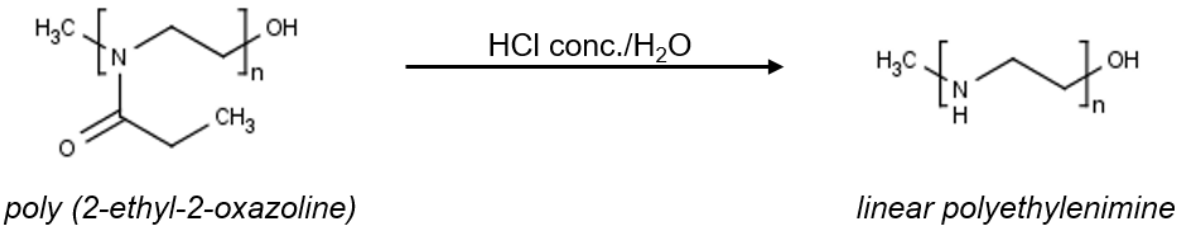

poly (2-ethyl-2-oxazoline) *linear polyethylenimine*

A big advantage of LPEI is the chemical modifiability such as adding compounds like peptides for targeting specific sites of tumour cells (Schaffert, 2013). GE11 is an oligopeptide with an affinity to epidermal growth factor receptor, without activating the kinase activity which would lead to extended tissue growth. Polyplexes modified with GE11 are targeted to EGFR overexpressing tissues like many tumour types(Schafer, 2011).

For this purpose, the N-terminal L-cysteine of GE11 is linked via a heterobifunctional linker (NHS-PEG-OPSS) to LPEI. We adapted the protocol for LPEI-PEG-OPSS synthesis from Rödl et al (detailed reaction mechanism in Figure 34) (Rodl, 2013).

Figure 34 *Reaction between LPEI and the bifunctional NHS-PEG-OPSS linker; N-hydroxysuccinimide (NHS) is the cleavage product of this reaction*

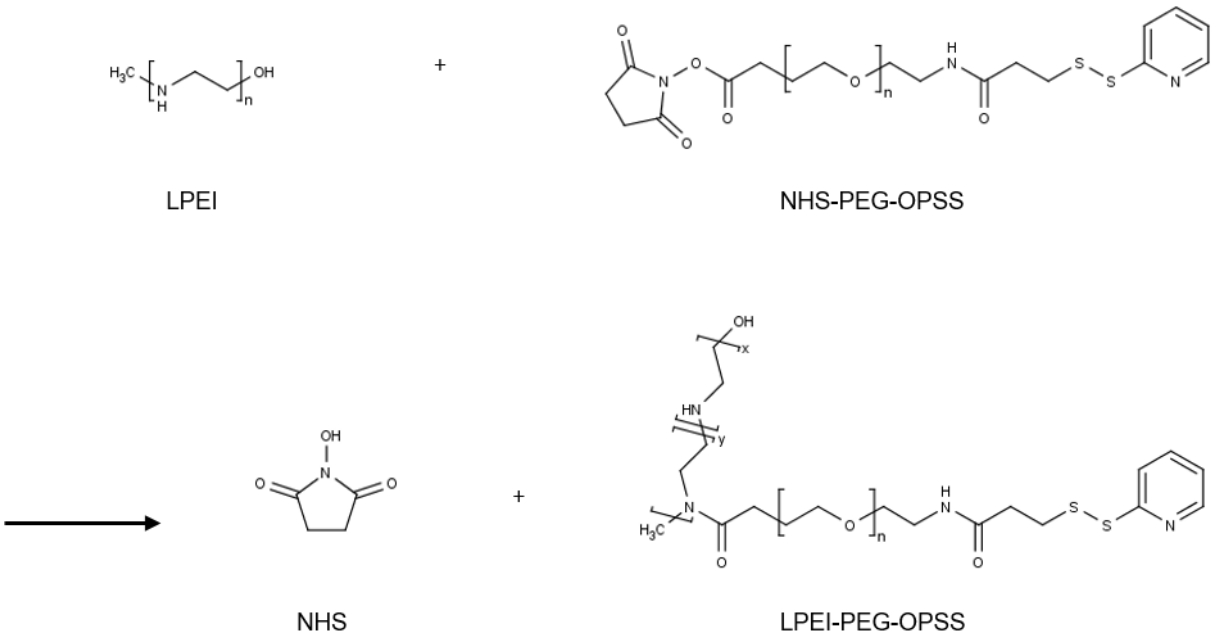

Although the protocol of Rödl et al. described the coupling of GE11 with the LPEI-PEG-OPSS conjugate, we chose to use L-cysteine for optimizing the procedure since the reaction mechanism remains the same. Instead of 3.4 µmol LPEI we used 4.54 µmol (45.40 mg) of LPEI (10 kDa). Instead of 5 eq. (17 µmol), we used a twofold surplus of NHS-PEG-OPSS (18.60 mg; 2 eq.), since a molar ratios of PEG/LPEI between 0.8:1 and 1.5:1 are enough for efficient coupling (Schafer, 2011).

In Figure 35 the detailed reaction mechanism of the coupling of L-cysteine to LPEI-PEG-OPSS is depicted.

Figure 35 *Reaction mechanism of LPEI-PEG-Cysteine synthesis; thiopyridone is the cleavage product of the reaction; its absorption at 343 nm can be used as in process control*

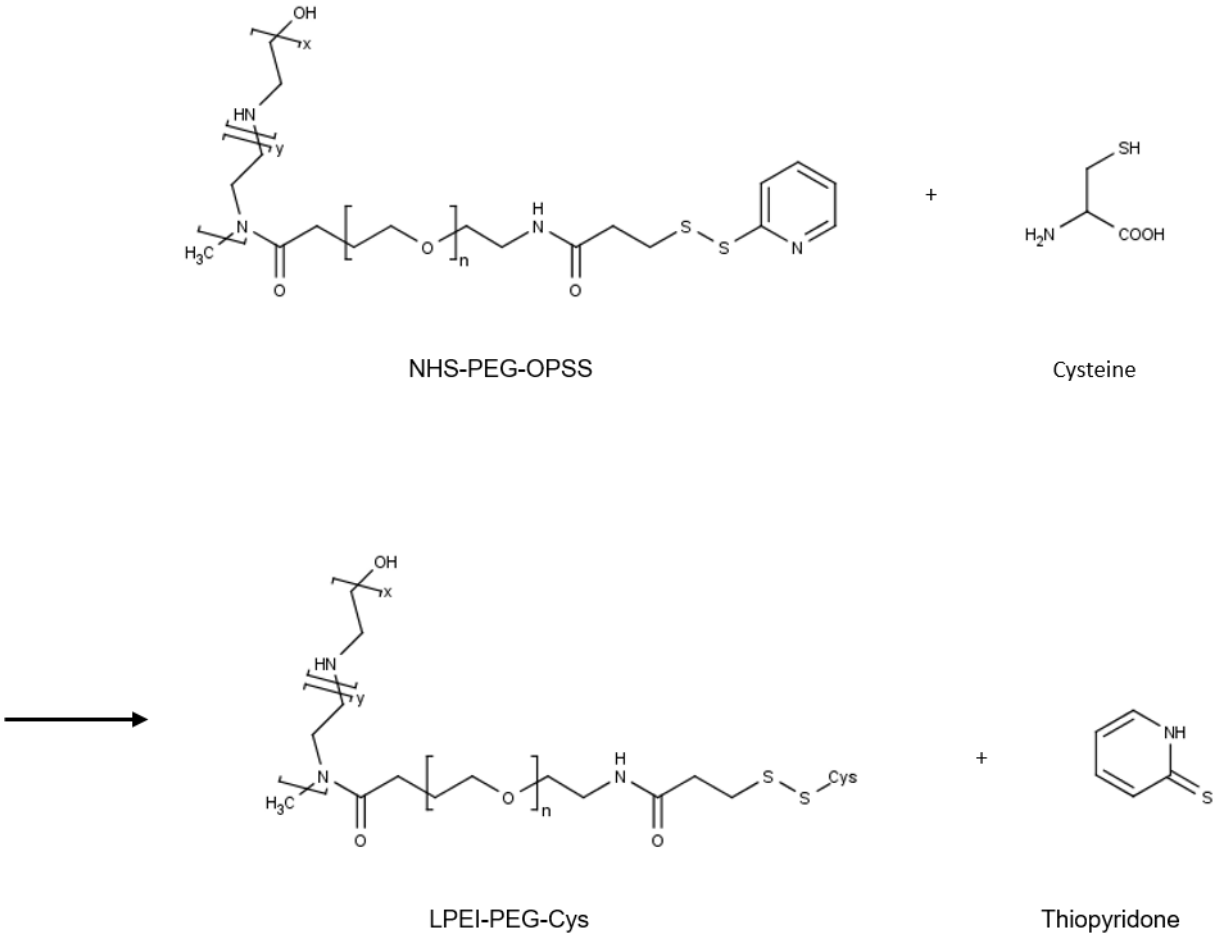

5.2 Investigation of biophysical properties of polyplexes

A centerpiece of this thesis was the investigation of biophysical properties like size and ζ-potential of polyplexes by nanoparticle tracking analysis (NTA) which gives measurements characterized by higher resolution when compared to other commercially available systems such as DLS based systems (Filipe, 2010).

We specifically investigated the impact of N/P ratio on size and ζ-potential, as these characteristics are known for influencing transfection efficiency as well as cytotoxicity (Behr, 1989; Boussif, 1995; Poulain, 2000; Boeckle, 2004).

Although N/P-ratios of 6 and 7.5 showed an increased size which does not agree with previously conducted studies the overall tendency of polyplexes is to get smaller when increasing the N/P ratio and hence being within a size range between 100 and 200 nm, where polyplexes are shown to have the best transfection efficiency *in vivo (Wightman, 2001)*. ζ-potential increased with the N/P-ratio. This may result in an increased interaction with negatively charged cellular membrane surface at higher N/P-ratios explaining higher transfection efficiency compared to polyplexes generated at lower N/P-ratios. However, a high N/P ratio also results in increased cytotoxicity due to non-specific ionic interaction of LPEI with the cellular membrane leading to breakdown of the membrane potential, reduction of cytoplasmic proteins and thus cell death (Fischer, 2003; Boeckle, 2004; Regnstrom, 2006; Breunig, 2007; Schaffert, 2013).

However, for efficient transfection and N/P-ratio of at least 5 is required, where a significant amount of free polyethylenimine is in solution (Boeckle, 2004).

The size of polyplexes increased with the pDNA concentration which was also observed elsewhere (Kasper, 2011).

Polyplexes based on pDNA and LPEI require fresh prior-to-use preparation due to their instability and tendency to aggregate in suspension (Rodl, 2013). Hence, we wanted to investigate the influence of incubation time on polyplex size to determine the stability of polyplexes. We observed an increase in size till an incubation time of 20 minutes. Surprisingly, polyplexes started to get smaller from 20 minutes onwards. This could be due to precipitation of the bigger aggregates that evolved during the time. These precipitates cannot be measured with NTA, which means they are no longer available for measurement, unlike the remaining smaller particles.

The standard method for polyplex preparation is mixing equal volumes of LPEI and pDNA containing solutions by flash pipetting. Unfortunately, this circumstance results in batch-to-batch variability. Furthermore, this method is limited to relatively low volumes. Hence, we optimized an up-scaled, more reproducible synthesis method for generating polyplexes using a syringe pump which was described by Kasper et al. (Kasper, 2011).

Our NTA measurements showed no significant difference between hand- and syringe pump made polyplexes regarding their size. A significant advantage regarding polydispersity of polyplexes made by the up-scaled method might be observed at higher plasmid concentrations, according to Kasper et al. They showed that polydispersity and size of polyplexes made by syringe pump method compared to pipette made polyplexes were similar at a pDNA concentration of 20 µg/ml, while polydispersity index of pipette made polyplexes made with a plasmid concentration of 400 µg/ml differed significantly from polyplexes made by syringe pump with the same plasmid concentration (Kasper, 2011).

To simulate circumstances in cell culture, we investigated the size of polyplexes diluted in different media, since there is no relevant data regarding this specific topic published yet. Polyplexes were diluted in HBG and RPMI 1640, respectively. Especially at N/P-ratio of 9 polyplexes diluted in RPMI 1640 were significantly bigger. This might also affect the transfection efficiency.

The fact that salt concentration of the in the synthesis buffer used for polyplex generation has an influence on aggregation behaviour and transfection efficiency is already described in literature (Ogris, 1998; Wightman, 2001). Polyplexes formed in salt containing environment sometimes show better transfection efficiency *in vitro* compared to polyplexes generated under salt free conditions. On the other hand polyplexes formed in salt free media show better transfection efficiency *in vivo (Wightman, 2001)*.

The reason for this phenomenon may lie in aggregation behaviour: while polyplexes generated in salt free environment stay rather small, polyplexes formed in salt containing media such as HBS show aggregation which leads to polyplexes settling down onto cells in culture resulting in higher *in vitro* transfection efficiency. On the other hand, this aggregation hampers the distribution, cellular uptake and therefore transfection efficiency *in vivo (Behr, 1989)*.

Furthermore, we generated fluorescently labelled polyplexes for analyzing changes in the particle properties in complete medium which contains fetal calf serum (FCS). The serum proteins would be detected by NTA and therefore disturb the whole measurement. NS500 is equipped with a fluorescence filter and hence is able to visually distinguish between fluorescently labelled particles from FCS derived particles. (http://www.malvern.com/de/products/product-range/nanosight-range/nanosight-ns500/default.aspx, 2015).

Thus, LPEI was fluorescently stained with fluorescein isothiocyanate (FITC) in order to distinguish the FITC-LPEI based polyplexes from particles of the media. Unfortunately, the fluorescent emission delivered by FITC bleached rather quickly when exposed to the laser of the NS500. Thus, an alternative fluorescent staining has to be found. The reaction mechanism of the staining process is depicted in Figure 36.

Figure 36 *Reaction scheme of FITC labelling of LPEI*

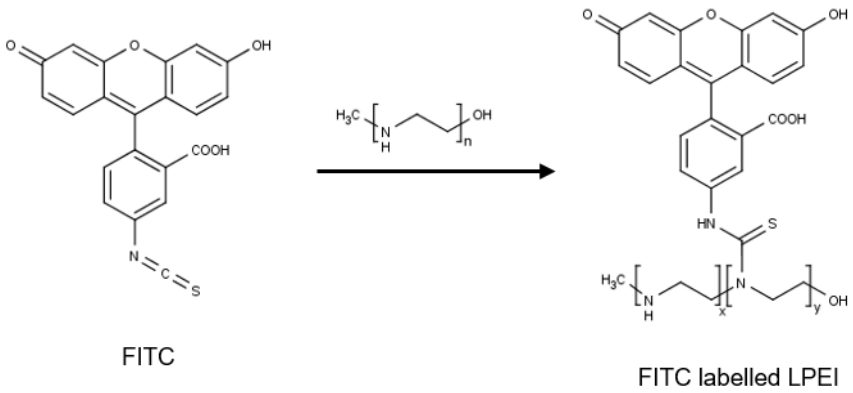

6 Appendix

6.1 Abstract

Linear polyethylenimine (LPEI) is amongst the most important non-viral vector for gene therapy. The chemical modifiability of this polymer like the possibility of introducing targeting moieties is making it a versatile tool for gene therapy. Mixed with nucleic acids nanoparticles, so-called polyplexes, are formed due to electrostatic interactions followed by hydrophobic collapse. These nanoparticles are able to transfect cells by adsorptive endocytosis.

We synthesized poly(2-ethyl-2-oxazolines) of four different molar weights using 2-ethyl-2-oxazoline as initial compound. Via acidic hydrolysis linear polyethylenimine was generated. In place of GE11, a targeting peptide which couples with the EGF receptor without activating it LPEI was modified with L-cysteine using a heterobifunctional PEG linker.

Polyplexes were generated by mixing solutions of LPEI and plasmid DNA (pDNA) by flash pipetting.

An important task of this thesis was the investigation of size and ζ-potential by nanoparticle tracking analysis (NTA) since these properties directly correlate with the transfection efficiency and toxicity of polyplexes.

Our results showed that an increase of the LPEI to plasmid ratio leads to a decrease of size and an increase of ζ-potential. Polyplexes generated with an N/P-ratio of 3 had no kinetic stability. An increase of pDNA concentration and incubation time led to an increase of the average diameter of the particles.

Also the dilution buffer has influence on size. Polyplexes (generated in HEPES buffered Glucose (HBG)) were diluted in HBG and RPMI 1640, respectively. The measurements revealed that especially at N/P-ratio of 9 polyplexes diluted in RPMI 1640 were significantly bigger than those diluted in HBG.

Furthermore, polyplex properties are also dependent on the buffer system used during nanoparticle generation. Polyplexes generated in HEPES buffered saline showed increased aggregation and therefor size, compared with polyplexes generated in HBG.

Moreover, an up-scaled, more reproducible method of polyplex formation was optimized. For this purpose, a syringe pump was employed, since the flowrate and syringe size is adjustable.

6.2 Zusammenfassung

Lineares Polyethylenimin (LPEI) gehört zu den wichtigsten nicht-viralen Gentransfervektoren. Die chemische Modifizierbarkeit des Polymers, wie etwa die Möglichkeit der Einführung von Targeting-Einheiten macht es zu einem vielseitigen Werkzeug für die Gentherapie. Mischt man LPEI mit Nukleinsäuren, bilden sich durch elektrostatische Wechselwirkungen gefolgt von einem hydrophoben Kollaps Nanopartikel, sogenannte Polyplexe. Diese Nanopartikel können Zellen durch adsorptive Endozytose und die Freisetzung von DNA innerhalb der Zelle transfizieren.

Wir synthetisierten Poly(2-ethyl-2-oxazoline) vier verschiedener Molekulargewichte unter der Verwendung von 2-Ethyl-2-oxazolin als Ausgangssubstanz. Mittels saurer Hydrolyse wurde lineares Polyethylenimin synthetisiert. Anstelle von GE11, ein Targeting-Peptid, das an den EGF-Rezeptor bindet ohne ihn dabei zu aktivieren wurde LPEI mithilfe eines heterobifunktionellen PEG-Linkers mit L-Cystein modifiziert.

Polyplexe wurden durch Mischen von LPEI und Plasmid DNA (pDNA) Lösungen und anschließendem „Flash-Pipetting“ hergestellt.

Ein wichtiger Punkt dieser Arbeit war die Untersuchung der Größe und des ζ-Potentials der Nanopartikel mittels der Nanopartikel-Tracking-Analyse (NTA), da diese Eigenschaften direkt mit der Transfektionseffizienz und Toxizität von Polyplexen korrelieren.

Unsere Ergebnisse zeigten, dass eine Erhöhung des LPEI zu Plasmid Verhältnis zu einer Abnahme der Größe und einer Erhöhung des ζ-Potentials führt. Polyplexe erzeugt bei einem N/P-Verhältnis von 3 hatten keine kinetische Stabilität. Eine Erhöhung der pDNA Konzentration und der Inkubationszeit führte zu einer Erhöhung des durchschnittlichen Durchmessers der Partikel.

Auch der Verdünnungspuffer hat Einfluss auf die Größe. Polyplexe (erzeugt in HEPES-gepufferter Glucose (HBG)) wurden jeweils in HBG und RPMI 1640, verdünnt. Die

Messungen ergaben, dass insbesondere bei einem N/P-Verhältnis von 9 Polyplexe verdünnt in RPMI 1640 deutlich größer waren als diejenigen in HBG verdünnt.

Weiterhin sind Polyplex Eigenschaften auch abhängig vom Puffersystem, das während Nanopartikelerzeugung verwendet wird. Polyplexe, die in HEPES-gepufferter Salzlösung erzeugt wurden zeigten vermehrt Aggregatbildung, die Partikel waren im Durchschnitt dadurch größer, verglichen mit Polyplexen, die in HBG hergestellt wurden.

Darüber hinaus optimierten wir ein hochskalierbares, besser reproduzierbares Verfahren zur Polyplex Herstellung. Zu diesem Zweck wurde eine Spritzenpumpe eingesetzt, da sowohl Strömungsgeschwindigkeit und die Spritzengröße einstellbar sind.

7 References

Akhtar, S. (2006). Non-viral cancer gene therapy: beyond delivery. Gene Ther **13**(9): 739-740.

Behr, J. P., Demeneix, B., Loeffler, J. P., et al. (1989). Efficient gene transfer into mammalian primary endocrine cells with lipopolyamine-coated DNA 6. Proc.Natl.Acad.Sci.U.S.A **86**(18): 6982-6986.

Boeckle, S., von Gersdorff, K., van der Piepen, S., et al. (2004). Purification of polyethylenimine polyplexes highlights the role of free polycations in gene transfer. J Gene Med **6**(10): 1102-1111.

Boussif, O., Lezoualc'h, F., Zanta, M. A., et al. (1995). A versatile vector for gene and oligonucleotide transfer into cells in culture and in vivo: polyethylenimine. Proc.Natl.Acad.Sci.U.S.A **92**(16): 7297-7301.

Breunig, M., Lungwitz, U., Liebl, R., et al. (2007). Breaking up the correlation between efficacy and toxicity for nonviral gene delivery. Proc.Natl.Acad.Sci U.S.A **104**(36): 14454-14459.

Brissault, B., Kichler, A., Guis, C., et al. (2003). Synthesis of linear polyethylenimine derivatives for DNA transfection. Bioconjug.Chem. **14**(3): 581-587.

Carr, R., Hole, P., Malloy, A., et al. (2008). The real-time, simultaneous analysis of nanoparticle size, zeta potential, count, asymmetry and fluorescence.

Chollet, P., Favrot, M. C., Hurbin, A., et al. (2002). Side-effects of a systemic injection of linear polyethylenimine–DNA complexes. The journal of gene medicine, **4**(1), 84-91.

Chujo, Y., Sada, K., Matsumoto, K., et al. (1990). A novel nonionic hydrogel from 2-methyl-2-oxazoline. Synthesis of nonionic hydrogel, lipogel, and amphigel by copolymerization of 2-oxazolines and a bisoxazoline. Macromolecules **23**(5): 1234-1237.

Collet, G., Grillon, C., Nadim, M., et al. (2013). Trojan horse at cellular level for tumor gene therapies. Gene **525**(2): 208-216.

Cotrim, A. P. and Baum, B. J. (2008). Gene Therapy: Some History, Applications, Problems, and Prospects. Toxicologic Pathology **36**(1): 97-103.

Fernandez, C. A. and Rice, K. G. (2009). Engineered Nanoscaled Polyplex Gene Delivery Systems. Molecular Pharmaceutics **6**(5): 1277-1289.

Filipe, V., Hawe, A. and Jiskoot, W. (2010). Critical Evaluation of Nanoparticle Tracking Analysis (NTA) by NanoSight for the Measurement of Nanoparticles and Protein Aggregates. Pharm Res **27**(5): 796-810.

Fischer, D., Li, Y., Ahlemeyer, B., et al. (2003). In vitro cytotoxicity testing of polycations: influence of polymer structure on cell viability and hemolysis. Biomaterials **24**(7): 1121-1131.

Gehrig, S., Sami, H. and Ogris, M. (2014). Gene therapy and imaging in preclinical and clinical oncology: recent developments in therapy and theranostics. Ther Deliv: 1275-1296.

Hochwimmer, G., Nuyken, O. and Schubert, U. S. (1998). 6,6 '-bisfunctionalized 2,2 '-bipyridines as metallo-supramolecular initiators for the living polymerization of oxazolines. Macromolecular Rapid Communications **19**(6): 309-313.

Hoogenboom, R., Fijten, M. W. M., Brandli, C., et al. (2003). Automated parallel temperature optimization and determination of activation energy for the living cationic polymerization of 2-ethyl-2-oxazoline. Macromolecular Rapid Communications **24**(1): 98-103.

http://www.malvern.com/de/products/product-range/nanosight-range/nanosight-ns500/default.aspx (entered 12.10.2015)

http://www.malvern.com/de/products/product-range/zetasizer-range/zetasizer-nano-range/zetasizer-nano-zsp/default.aspx (entered 12.10.2015)

http://www.who.int/mediacentre/factsheets/fs297/en/ (entered 30.03.2016)

https://at.promega.com/resources/pubhub/enotes/how-do-i-determine-the-concentration-yield-and-purity-of-a-dna-sample/ (entered 16.12.2015)

Jones, G. D., Langsjoen, A., Neumann, M. M. C., et al. (1944). The polymerization of ethylenimine. Journal of Organic Chemistry **9**(2): 125-147.

Kasper, J. C., Schaffert, D., Ogris, M., et al. (2011). The establishment of an up-scaled micro-mixer method allows the standardized and reproducible preparation of well-defined plasmid/LPEI polyplexes. Eur J Pharm Biopharm **77**(1): 182-185.

Kichler, A. (2004). Gene transfer with modified polyethylenimines. J Gene Med **6** S3-S10.

Kircheis, R., Wightman, L., Schreiber, A., et al. (2001). Polyethylenimine/DNA complexes shielded by transferrin target gene expression to tumors after systemic application. Gene Ther **8**(1): 28-40.

Klug, W. S. C., M. R.; Spencer, C. A. (2012). Concepts of genetics. Pearson Education **10**.

Klutz, K., Russ, V., Willhauck, M. J., et al. (2009). Targeted radioiodine therapy of neuroblastoma tumors following systemic nonviral delivery of the sodium iodide symporter gene. Clinical Cancer Research, **15**(19), 6079-6086.

Li, Z., Zhao, R., Wu, X., et al. (2005). Identification and characterization of a novel peptide ligand of epidermal growth factor receptor for targeted delivery of therapeutics. Faseb J **19**(14): 1978-1985.

Lio, P. and Vannucci, M. (2000). Finding pathogenicity islands and gene transfer events in genome data. Bioinformatics **16**(10): 932-940.

Litt, M., Levy, A. and Herz, J. (1975). Polymerization of Cyclic Imino Ethers .10. Kinetics, Chain Transfer, and Repolymerization. Journal of Macromolecular Science-Chemistry **A 9**(5): 703-727.

Lungwitz, U. (2006). Polyethylenimine-derived gene carriers and their complexes with plasmid DNA (Design, Synthesis and Characterization). Faculty of Chemistry and Pharmacy; University of Regensburg.

Magnusson, T., Haase, R., Schleef, M., et al. (2011). Sustained, high transgene expression in liver with plasmid vectors using optimized promoter-enhancer combinations. The journal of gene medicine, **13**(7-8), 382-391.

Matissek, K. J. B., R. R.; Davis, J. R. (2011). Choosing Targets for Gene Therapy. INTECH Open Access Publisher.

Miyamoto, M., Aoi, K. and Saegusa, T. (1988). MECHANISMS OF RING-OPENING POLYMERIZATION OF 2-(PERFLUOROALKYL)-2-OXAZOLINES INITIATED BY SULFONATES - A NOVEL COVALENT-TYPE ELECTROPHILIC POLYMERIZATION. Macromolecules **21**(6): 1880-1883.

Miyamoto, M., Aoi, K. and Saegusa, T. (1991). NOVEL COVALENT-TYPE ELECTROPHILIC POLYMERIZATION OF 2-(PERFLUOROALKYL)-2-OXAZOLINES INITIATED BY SULFONATES. Macromolecules **24**(1): 11-16.

Nguyen, J. and Szoka, F. C. (2012). Nucleic acid delivery: the missing pieces of the puzzle? Acc Chem Res **45**(7): 1153-1162.

Nuyken, O., Persigehl, P. and Weberskirch, R. (2002). Amphiphilic poly(oxazoline)s - Synthesis and application for micellar catalysis. Macromolecular Symposia **177**: 163-173.

Ogris, M., Steinlein, P., Kursa, M., et al. (1998). The size of DNA/transferrin-PEI complexes is an important factor for gene expression in cultured cells. Gene Ther **5**(10): 1425-1433.

Poulain, L., Ziller, C., Muller, C. D., et al. (2000). Ovarian carcinoma cells are effectively transfected by polyethylenimine (PEI) derivatives 1010. Cancer Gene Ther. **7**(4): 644-652.

Regnstrom, K., Ragnarsson, E. G. E., Fryknas, M., et al. (2006). Gene expression profiles in mouse lung tissue after administration of two cationic polymers used for nonviral gene delivery. Pharmaceutical Research **23**(3): 475-482.

Rinkenauer, A. C., Tauhardt, L., Wendler, F., et al. (2015). A Cationic Poly(2-oxazoline) with High In Vitro Transfection Efficiency Identified by a Library Approach. Macromolecular Bioscience **15**(3): 414-425.

Rödl, W., Schaffert, D., Wagner, E., et al. (2013). Synthesis of polyethylenimine-based nanocarriers for systemic tumor targeting of nucleic acids. Methods Mol Biol **948**: 105-120.

Schafer, A., Pahnke, A., Schaffert, D., et al. (2011). Disconnecting the Yin and Yang Relation of Epidermal Growth Factor Receptor (EGFR)-Mediated Delivery: A Fully Synthetic, EGFR-Targeted Gene Transfer System Avoiding Receptor Activation. Hum Gene Ther **22**(12): 1463-1473.

Schaffert, D. and Ogris, M. (2013). Nucleic Acid Carrier Systems Based on Polyethylenimine Conjugates for the Treatment of Metastatic Tumors. Current Medicinal Chemistry **20**(28): 3456-3470.

Su, B., Cengizeroglu, A., Farkasova, K., et al. (2013). Systemic TNFalpha gene therapy synergizes with liposomal doxorubicine in the treatment of metastatic cancer. Mol Ther **21**(2): 300-308.

Szybalska, E. H. and Szybalski, W. (1962). Genetics of human cess line. IV. DNA-mediated heritable transformation of a biochemical trait. Proc.Natl.Acad.Sci U.S.A **48**: 2026-2034.

Vogelstein, B. and Kinzler, K. W. (2004). Cancer genes and the pathways they control. Nat Med **10**(8): 789-799.

Wightman, L., Kircheis, R., Rossler, V., et al. (2001). Different behavior of branched and linear polyethylenimine for gene delivery in vitro and in vivo. J Gene Med **3**(4): 362-372.